ABSTRACT

Title of Dissertation: IMPACT OF LIPOPOLYSACCHARIDE ADMINISTRATION ON NOVEL RNA BIOMARKERS FOR SYSTEMIC INFLAMMATION IN SWINE

Trevon Brandon Swain, Doctor of Philosophy, 2020

Dissertation directed by: Theodore K. Dayie, Ph.D. Professor, Department of Chemistry and Biochemistry
&
Dr. Michael J. Myers, Ph.D. Deputy Division, Director
United States Food and Drug Administration

In veterinary medicine, inflammation in swine is evaluated solely by clinical signs. Due to the inconsistent interpretations of clinical observations between different clinicians, this method is often unreliable when assessing large animal populations. The lack of a validated swine animal model prevents an accurate measurement of inflammation and inhibits the development of new effective

veterinary drugs for swine. This study examined whether changes in protein and miRNA expression levels can predict the severity of the inflammatory response in swine after administration of lipopolysaccharide (LPS) from *Escherichia coli* (*E.coli*). Identification of a reliable biomarker from a systemic inflammatory response needs to be easily obtained, safe, and provide the lowest risk of discomfort to the subject. We demonstrated *in vivo* the involvement of several swine microRNAs (let-7e-5p, miR-22-3p, miR-146a and others) in systemic inflammatory responses. The correlation of the clinical signs with individual miRNA levels may establish a plasma biomarker that can determine the severity of inflammation in swine. The long-term goal is to determine the most powerful tool for analysis and biomarker discovery. Exploring the different methodologies and monitoring different miRNAs increases the likelihood for potential advancements in disease detection applications.

IMPACT OF LIPOPOLYSACCHARIDE ADMINISTRATION ON NOVEL RNA BIOMARKERS FOR SYSTEMIC INFLAMMATION IN SWINE

by

Trevon Brandon Swain

Dissertation submitted to the Faculty of the Graduate School of the
University of Maryland, College Park, in partial fulfillment
of the requirements for the degree of
Doctor of Philosophy
2020

Advisory Committee:
Professor Theodore K. Dayie, Chair
Dr. Michael J. Myers, Co-Chair
Associate Professor Nicole A. LaRonde-LeBlanc
Professor John Orban
Professor Wade C. Winkler

Preface

This research work was supported by the U.S. Food and Drug Administration's Center for Veterinary Medicine (CVM) in the Division of Applied Veterinary Research (DAVR). The following dissertation provides preliminary evidence for the drug development industry to assess the efficacy of drugs that have claims to treat inflammation in a validated swine animal model. The goal of this research is to identify changes in miRNA expression that can predict the severity of the inflammatory response in swine after administration of *Escherichia coli* lipopolysaccharide (LPS).

Dedication

This dissertation is dedicated to my family and many friends. A special feeling of gratitude for my loving parents, Anthony and Joy Swain, whose support and words of encouragement do not go unnoticed. I dedicate this to all my friends and family that have supported me throughout this entire process over the years. Finally, I also dedicate this work and give special thanks to my wife, Tiffani Swain, for providing love and support every step of the way.

Acknowledgements

I would like to express my gratitude to the Food and Drug Administration Center for Veterinary medicine for supporting and funding my research work over the years. I thank the staff members in the DAVR, especially the Animal Care team, for their support and assistance. I especially would like to thank Dr. Michael Myers for agreeing to be my off-campus advisor and helping me become a better research scientist. Dr. Myers has spent hours reviewing and providing writing advice, challenging me to communicate my research effectively, and I am forever thankful to him.

I thank Dr. Michael Myers, Dr. Theodore Dayie, Dr. Nicole A. LaRonde-LeBlanc, Dr. John Orban, and Dr. Wade C. Winkler for being on my thesis committee and constantly providing feedback on my research. I would also like to thank all the group members in Dr. Dayie's lab group, past and present, for all their constructive criticism on presentations as well as hours spent reading drafts of manuscripts and papers for my benefit.

Finally, I want to thank my wife and family for always being supportive and help care for baby Teagan while I wrote this dissertation.

Any omission in these Acknowledgments does not mean a lack of appreciation, gratitude, or recognition.

Table of Contents

List of Tables

List of Figures

List of Illustrations

List of Abbreviations

1-DGE	One-dimensional gel electrophoresis
2-DGE	Two-dimensional gel electrophoresis
APPs	Acute phase proteins
BSA	Bovine serum albumin
C. elegans	Caenorhabditis elegans
CID	Collision-induced dissociation
CLP	Cecal ligation and puncture
Ct	Cycle threshold
CVM	Center for Veterinary Medicine
DAD1	Defender Against Cell Death 1
DAVR	Division of Applied Veterinary Research
E.coli	Escherichia coli
ELISA	Enzyme-linked immunosorbent assay
ESR1	Estrogen Receptor 1, Estrogen Receptor 1
HDAC4	Histone Deacetylase 4
IRAK1	IL-1R-associated kinase 1
LPS	Lipopolysaccharide
NF- κβ	Nuclear Factor κβ
nLC-MS/MS	Nano-liquid chromatography coupled with tandem mass spectrometry

NSAIDs	Non-steroidal anti-inflammatory drugs
nt	nucleotide
PBS	Phosphate-buffered saline
PCI	Peritoneal contamination and infection
PDSI	Personal densitometer SI
PGE2	Prostaglandin E2
Poly I:C	Polyinosinic:polycytidylic acid
qRT-PCR	Quantitative real-time-PCR
SELDI-TOF	Surface-enhanced laser desorption ionization time-of-flight
SEM	Standard error of the mean
SIRS	Systemic inflammatory responses syndrome
SIRT1	Sirtuin 1
TLR2	Toll-like receptor 2
TLR4	Toll-like receptor 4
TRAF6	Tumor necrosis factor receptor -associated factor 6
TXB2	Thromboxane B2

Chapter 1: General Introduction

There are no FDA-approved non-steroidal anti-inflammatory drugs (NSAIDs) for the control of inflammation in swine. Flunixin meglumine (Banamine®) is the only FDA-approved NSAID on the pharmaceutical market for animals used for food production or for human consumption. In cattle, the approved claims are the control of fever and inflammation in endotoxemia. The control of inflammation claim was based on the reduction of prostaglandin E2 (PGE2) and thromboxane B2 (TXB2) synthesis (Anon, 2004). However, the impact of flunixin on PGE2 production in cattle was demonstrated using an endotoxin-induced model of inflammation rather than actual clinical cases. In swine, flunixin is only approved for the control of pyrexia (Peters et al., 2012). In human medicine, the reduction in prostaglandin E2 has been the standard measure to determine a NSAIDS's ability to control inflammation (Ricciotti & FitzGerald, 2011). In contrast, the veterinary pharmaceutical industry has claimed to the US FDA, Center of Veterinary Medicine, that PGE2 changes cannot be measured in food animals such as cattle and swine during clinical efficacy trials (Myers, Scott, Deaver, Farrell, & Yancy, 2010). This suggested that it was either too difficult to measure PGE2, it was not produced in enough quantities in circulation to be detected, or that it was not produced at a time when clinical signs were evident. Since there are numerous studies demonstrating the production peak of PGE2 in swine (Klosterhalfen et al., 1991; Peters et al., 2012), it would seem that the production and detection of PGE2 is not the issue. Rather, it may

be one of the timing of detection. During clinical trials conducted by pharmaceutical sponsors to demonstrate drug efficacy, animals are not enrolled into the study until they exhibit clinical signs of disease or infection. Therefore, under those restrictions, it is probable that production of PGE2 has peaked prior to study enrollment and a biomarker that remains in circulation for a longer period is necessary. The lack of a validated reproducible swine model for inflammation prevents an accurate measurement of NSAID efficacy, therefore inhibiting the development of effective NSAIDs for swine. The problems associated with the absence of a validated animal model are further compounded by the absence of qualified surrogate endpoints to assess NSAID efficacy in controlling inflammation. This study evaluates changes in plasma protein and miRNA biomarkers as a reliable means to assess the severity of inflammation in swine. The long-term goal is to determine the most powerful tool for analysis and biomarker discovery. Exploring the different methodologies and monitoring different molecules increases the likelihood for potential advancements in disease detection applications.

Chapter 2: Literature Review

Biomarkers

The ability to assess the severity of inflammation in swine is significant to veterinary medicine. Currently, the assessment of clinical signs, such as temperature, respiration rate, and heart rate, are the most widely used approaches for determining the inflammation status of swine. However, evaluating the health status of the animals using clinical signs alone is not enough for determining the effectiveness of potential drug therapies with claims to control inflammation. Assessing and controlling diseases in a swine production environment is of great importance for overall health and welfare and achieve a better quality of product. Disease control in swine continues to gain attention in veterinary research due to financial losses and a general concern for food safety. There are no established clinical signs or laboratory measures that can substantiate a claim of control of inflammation in swine. Therefore, useful and practical biological indicators are needed on farms and in veterinary medicine in general to assess livestock on a large scale. Biological markers measure normal biologic processes, pathogenic processes, or pharmacologic responses to a therapeutic intervention ("Biomarkers and surrogate endpoints: preferred definitions and conceptual framework," 2001).

There are different types of biomarkers, such as predictive, diagnostic, prognostic, and pharmacodynamic biomarkers, which may be utilized in a variety of applications (Millner & Strotman, 2016). The use of a biomarker could range from the identification to assessing the severity to the disease probability of recurrence. A biomarker can also be a measurement that reflects an interaction between a biological system and a potential hazard, which may be chemical, physical, or biological with a measured response according to the World Health Organization (Strimbu & Tavel, 2010). It is important to note that not all biomarkers are useful in practice, especially if the measurable biological characteristic negatively affects the morbidity or mortality of the subject. However, clinical endpoints take into consideration the overall health of the subject, and specifically measures the outcomes of how a subject feels, functions, and survives ("Biomarkers and surrogate endpoints: preferred definitions and conceptual framework," 2001). Additionally, clinical endpoints such as death or recurrence after many years, may not be practical endpoints for a drug study design which could ultimately hinder treatment availability for targeted subjects. In veterinary medicine, surrogate endpoints, which could be a safe biomarker from the subject, can substitute for but should not replace a clinical endpoint. There must be scientific evidence, coupled with the accurate and consistent prediction of a clinical outcome, to be considered a surrogate endpoint by a biomarker (Strimbu & Tavel, 2010). Surrogate endpoints may shorten the required time for drug approval for certain drugs as well as expand the veterinary drug discovery and development process.

Proteins, antibodies, metabolites, and RNA are common types of biomarkers used for drug development, disease predictors, and detectors. Ideally, a biomarker should be easy to obtain, safe, and provide the lowest risk of discomfort to the subject (van Bragt et al., 2018). Traditionally, urine and blood sample types are commonly used to meet these characteristics. Determining if the detection method can be reproducible, specific, and sensitive to the biomarker is of high importance. While all strategies have their limitations, the advantages of using circulating biomarkers as a tool for screening and early detection for inflammation will be highlighted as a reliable method.

Proteomics and microRNAs

Proteomics is the field of molecular biology that is focused on the large-scale study of proteins present in the body at any period (Wasinger et al., 1995). However, the study of proteins started even further back in 1975 with the two-dimensional electrophoresis (2-DGE) of *Escherichia coli* (O'Farrell, 1975). Although individual proteins could not be identified, this method could visualize the separation of several proteins. A key to proteomics is understanding that any given proteome is dynamic because proteins can be altered, modified, or degraded by several different mechanisms for regulation, including the inflammatory process (Ito, 2007). Therefore, the proteome of a cell or an organism is only at the specific protein environment at the time point being studied. The overall objective of proteomics is to study the global changes of all the proteins compared to protein changes observed in

individual cells. Proteomics can characterize the expression of several proteins from multiple cells within the biofluid biological system simultaneously. Since a proteome can differ from cell to cell, taking consideration for its environment and changes will represent the total impact.

Comparative proteomics analyzes changes in the proteome from responses such as diseases or environment (Minden, 2007). Responses from biological processes and outside stimuli can trigger expressions or suppressions of additional sets of proteins at different stages during the duration of each study. Capturing the different proteome profiles is important for understanding the total changes observed. Quantitative proteomics is an approach used for discovery and targeted proteomic analyses to determine the amount of proteins in a sample. A challenge associated with any comparative proteomic analysis is the complexity of the sample matrix. For example, serum albumin has been reported to account for more than half of the total protein concentration in plasma (Bandow, 2010).

One-dimensional electrophoresis (1-DGE) is useful for identifying the presence and abundance of different proteins in fluid samples. Molecule mixtures can be separated on a polyacrylamide gel. Protein molecules are typically not negatively charged. Therefore, applying the electric field may not necessarily separate proteins (Requião et al., 2017). However, treating protein mixtures with sodium dodecyl sulfate (SDS), denatures native proteins into a linear polypeptide and coats the protein with a uniform negative charge (Gudiksen, Gitlin, & Whitesides, 2006), enabling

consistent separation on applying an electric field. The distance the protein bands migrate on the gel can be correlated with their molecular weights (MWs).

As mentioned previously, 2-DGE is another form of gel electrophoresis technique that first separates protein molecules by their isoelectric points (pI), then by their molecular weight. It is a commonly used method for complex samples to increase the detection of low-abundance proteins that are undetectable in one dimensional gel electrophoresis (Gorg, Weiss, & Dunn, 2004). While there are several software platforms to analyze 2-DGE and compare expression levels between images of different samples, major disadvantages of any software-based gel image analysis include the co-migration of proteins on the gel itself and detection of weak or mismatched spots.

Additionally, combining 2-DGE to separate hundreds of proteins from a sample in a single gel with an in-gel digestion technique allows for protein identification using mass spectrometry (Person et al., 2006). Spot excision on the gel, destaining the gel spots, reduction, alkylation, protein breakdown to smaller polypeptides by digestion, and the protein extraction are the general steps involved in a typical in-gel digestion protocol (Gorg et al., 2004). The removal of salts, detergents, and impurities is another purification step to improve the extractions of proteins from the gel matrix. The peptide mixture is then sent for further analysis by selecting the optimum mass spectrometry instrument for the sample. There are several different proteins with a variety of functions and roles within a host. Thus, the analysis outlined above can allow us to follow changes in the swine plasma proteome

over the course of administering a drug, and the results will provide insights into the expression of potential useful diagnosis protein biomarkers.

In addition to proteomic analysis, one can also use RNAs, specifically microRNAs that are non-protein coding RNAs. The first non-protein-encoding RNA (ncRNA) lin-4, was discovered in *Caenorhabditis elegans* (*C. elegans*) and lin4 expression was correlated with decreased LIN-14 protein levels (Lee, Feinbaum, & Ambros, 1993; Wightman, Ha, & Ruvkun, 1993). Prior to the finding the lin-4 genes are ncRNAs, the knowledge of the roles of ncRNAs was limited and unknown (Bartel, 2018). These ~20-30 nucleotide small ncRNAs, dubbed microRNAs (miRNAs), inhibit translation or degrades mRNAs by binding to the 3′-untranslated regions (UTR), to coding sequences or 5′-UTR of messenger RNAs (mRNAs (Almeida, Reis, & Calin, 2011; Bartel, 2018). Recent studies of have uncovered their role and functions in many pathophysiological processes such as inflammation (Jiang, Zhang, & Shen, 2020; Moschos et al., 2007). In addition to down-regulating gene expression, miRNAs can activate transcription by binding to the promoter region of protein-coding genes (Dharap, Pokrzywa, Murali, Pandi, & Vemuganti, 2013).

Most miRNAs are synthesized typically through the canonical biogenesis pathway (Illustration 1). Primary miRNAs (pri-miRNAs) are transcribed by the RNA Polymerase II, and this transcript is cleaved into a ~55-70 nucleotide (nt) precursor miRNA (pre-miRNA) in the nucleus by Drosha and DGCR8 (also known as Pasha) microprocessor complex (Yang & Lai, 2011). The pre-miRNA, which has a 2-nt 3'-overhang, is then exported to the cytoplasm by an exportin 5 (XPO5) complex to be

processed by the Dicer RNase III endonuclease (Okada et al., 2009). However, in noncanonical miRNAs, the Drosha or Dicer enzymes are not involved in this alternative pathway (Abdelfattah, Park, & Choi, 2014). The 2-base 3'-overhang is necessary for efficient complex formation. The terminal loop is removed, and the mature miRNA duplex is formed in which the directionality of each miRNA strand provides the template for cleavage or suppression (H. Zhang, Kolb, Jaskiewicz, Westhof, & Filipowicz, 2004). The Argonaute (AGO) family of proteins loads both strands and the strand with the lower 5' thermodynamic stability, which is considered the guide strand, remains loaded in the AGO (O'Brien, Hayder, Zayed, & Peng, 2018). The unloaded strands, known as the passenger strand, are then unwound from the duplex, released, and cleaved by AGO2 and then degraded (Ha & Kim, 2014). Gene regulation can be achieved with the miRNA-induced silencing complex (miRISC) in which AGO bound to the guide strand interacts with complementary sequences on target mRNAs to repress protein synthesis or degrade the mRNA (Pratt & MacRae, 2009). Previous studies have proposed that different miRNA mechanism of actions are not only based on kinetics of miRNA or target mRNA but also on different cell types and specific mRNA targets (Jin & Xiao, 2015). Understanding the different methods of gene targeting by miRNAs and mechanisms of action is essential for using these molecules therapeutically and in biotechnology.

Bioinformatics methods are used extensively in miRNA research to predict miRNA targets from over 270 organisms, and biochemical methods are used to validate these predictions. These established and validated targets are deposited in

databases such as miRbase and miRDB (Y. Chen & Wang, 2020; Kozomara, Birgaoanu, & Griffiths-Jones, 2018). Using deposited miRNA binding and targeting expression data, a target prediction algorithm can provide potential evidence for the biological functions of these miRNAs. The prediction of miRNA targets for plants has been effective because the target mRNA and miRNA are typically perfectly complementary (Brennecke, Stark, Russell, & Cohen, 2005). This full or near perfect pairing, with no more than one mismatch in the 5' region has been known to lead to the degradation of mRNA (J. Wang, Mei, & Ren, 2019). However, in animals, typically positions 2-7 known as the seed region in the miRNA, matches to the mRNA 3' UTR for effective site pairing (Bartel, 2018). The partial complementarity of miRNA to mRNA in animals inhibits protein translation.

In recent years, microRNAs have played a role in gene expression during post-transcription regulation; these noncoding RNA molecules have been found in highly stable environments in serum and plasma (Carthew & Sontheimer, 2009; Kroh, Parkin, Mitchell, & Tewari, 2010). These miRNAs are found either bound to proteins such as AGO2 or within vesicles that protect them (Gallo, Tandon, Alevizos, & Illei, 2012). Extracellular miRNAs can be delivered to target cells and exhibit hormone-like functions and cell signaling (Iftikhar & Carney, 2016). These circulating miRNAs may be at sites undergoing cell death or injury in which the miRNAs are released into extracellular fluids (Turchinovich, Weiz, & Burwinkel, 2012).

The measurement of the circulating cell-free form of miRNA may have its challenges due to processing, extraction of RNA, and other technical issues. There are several different biochemistry techniques such as western blotting, luciferase reporter assays and polymerase chain reaction (PCR) than can assess the relationship between miRNA, mRNA, and proteins. Each technique has its own limitations and is dependent on the degree of quantitative and qualitative analysis needed for each experiment. In 1983 the idea of PCR was conceived by Dr. Kary Mullis which at the time was the process known as *in vitro* nucleic acid amplification (Schluger & Rom, 1995). This tool is used to amplify or copy small sequences of DNA or genes. The general technique is based on the ability for nucleotides, an appropriate buffer, and DNA polymerase to synthesize a strand of DNA from an existing DNA template strand (Valones et al., 2009). PCR involves three principal steps of denaturing, annealing, and extension during which the double stranded DNA is separated, the DNA primer attaches to the template DNA, and the new strand of DNA is synthesized (Valones et al., 2009). Real-time quantitative reverse transcriptase-polymerase chain reaction (qRT-PCR) method has allowed the quantification of nucleic acids with higher reproducibility, precision, and greater sensitivity. The PCR products are then detected by fluorescent dyes which are proportional to double-stranded DNA (dsDNA) or by a sequencing probe. SYBR Green is a dye that is only detectable when bound to dsDNA (Giglio, Monis, & Saint, 2003). The disadvantage of SYBR is that it can bind to any dsDNA which can lead to non-specific signals.

However, once optimized it is highly sensitive to a single molecule target within a reaction and can be used with multiple primers (Ponchel et al., 2003).

Quantitative RT-PCR has allowed researchers to quantify miRNA expression levels as a diagnostic method for detecting diseases in animals. Recently, researchers have aimed to understand host and virus miRNA roles by sequencing and expression profiling. Infected porcine PK-15 cell line showed down regulation in miR-92a and miR-92b-3p; the tissues collected from olfactory bulb (OB) or trigeminal ganglion (TG) *in vivo* experiment showed different expressions of miR-206, miR0133a, miR-133b in NIA-3 or Begonia viral strands (Timoneda et al., 2014).

Detecting which miRNAs are involved in mRNA gene expression can help researchers identify previously unknown functions and pathways in the posttranscriptional regulation process. Methods to confirm miRNA regulation of a gene can involve gene expression either reduced by a miRNA mimic or increased by a miRNA inhibitor. The transfection of chemically synthesized miRNA mimics or inhibitors into cells enables targets to be identified (Z. Wang, 2011). This study expands our understanding of host and viral miRNA in swine and use of miRNA biomarkers to differentiate a healthy from a diseased state. Establishing a relationship between expression of miRNA and the regulation of its targeted mRNA will be useful in characterizing a potential miRNA biomarker.

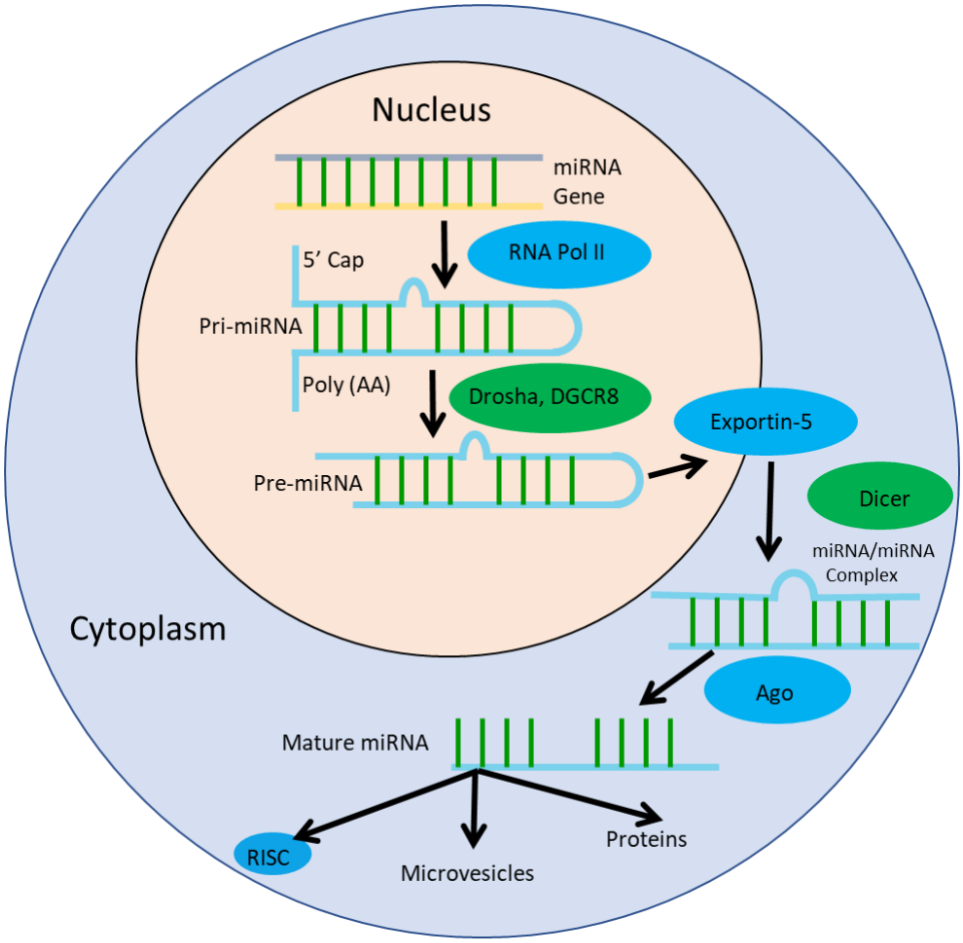

Illustration 1. The biogenesis of microRNAs in the canonical pathway. The primary miRNA transcript (pri-miRNA) is initially transcribed and cleaved near the hairpin structure into a precursor miRNA (pre-miRNA by the Drosha enzyme protein complex. The pre-miRNA is exported into the cytoplasm by Exportin-5 protein and then cut into duplex miRNA strands by the Dicer enzyme. The miRNA/miRNA complex with the 3' overhang (2nt) will be unzipped by the AGO protein and loaded into the RISC RNA-induced silencing complex for gene silencing and repression or packaged into microvesicles for cell to cell communication. *Note.* Adapted from *Frontiers in Physiology* by S. Asgari, 2011 (Asgari, 2011).

Systemic Inflammation

In 30-38 B.C., the clinical signs of redness (rubor), swelling (tumor), heat (calor), and pain (dolor) were coined to describe inflammation and about a century later loss of function was added to the definition (Punchard, Whelan, & Adcock,

2004). Until the 19th century, inflammation was considered harmful rather than beneficial to the host (Ryan & Majno, 1977). Inflammation, which can be trigged by physical and chemical signals from an injury, is part of a complex biological response. It is important to note that inflammation is usually associated with an infection. However, since an infection is caused by a microorganism and inflammation could be a response to the pathogen, not all infections necessarily show inflammation (Signore & Glaudemans, 2011).

The two major types of inflammations are acute, which can last a few days to weeks, and chronic, which can last a few months to years. Acute inflammation can be caused by circulating gram-negative bacterial such as lipopolysaccharide (LPS) in the blood (Kritselis et al., 2013). Different animal models that mimic systemic inflammation exist. Most of the models use techniques involving peritoneal contamination and infection (PCI) or cecal ligation and puncture (CLP), for instance; however, lipopolysaccharide (LPS) is preferable when observing the impact of acute inflammation (Seemann, Zohles, & Lupp, 2017). The presence of two or more abnormal clinical signs of a subject's core temperature, heart rate, respiratory rate, and leukocyte count as an inflammatory response is considered systemic inflammatory responses syndrome (SIRS), which can be caused by many different factors such as inflammation, ischemia, trauma, and infection (Gül, Arslantaş, Cinel, & Kumar, 2017).

Endotoxemia and SIRS have been induced by *E. coli*-derived lipopolysaccharide in many different species to date (Nemzek, Hugunin, & Opp,

2008). LPS is a cell wall component of gram-negative bacterium that contains three major components: the lipid A, core R polysaccharide, and O polysaccharide side chain (Maldonado, Sá-Correia, & Valvano, 2016). Lipid A is responsible for the toxicity of the bacterium which activates the Toll-like receptor 4 (TLR4) and triggers the pro-inflammatory signaling cascade. A sterile inflammation using LPS can induce endotoxemia which may mimic some septic responses. However, lipid A structures from *Rhodobacter sphaeroides* that may contain less than six fatty acyl groups may act as an LPS antagonist and can inhibit the activation of the TLR4 (Vargas-Caraveo et al., 2020).

The release of cytokines provided by this stimulation is responsible for the synthesis of acute phase proteins (APPs) in liver (Rossol et al., 2011). The result of the synthesis process may lead to establishing a relationship between APPs production in plasma with potential biomarkers based on alterations in gene expression. During inflammation, the concentration of this class of proteins can increase or decrease in the plasma. Major acute phase proteins, such as the Serum Amyloid A family of apolipoproteins, have concentrations in serum which increase up to 20-fold greater in the inflammatory state in swine (Pomorska-Mól et al., 2014). Unfortunately, the overwhelming presence of high abundance APPs can create difficulty identifying and measuring possible disease specific proteins of lower concentrations in plasma. It is important to note that strains of LPS derived from different bacteria may result in different responses due to recognition from various receptors such as Toll-like receptor 2 (TLR2) (Werts et al., 2001).

In swine, the inability to accurately assess the severity of inflammation with the use of biological indicators has prevented the validation of an animal model. Previously established animal models can be beneficial for predicting and comparing inflammatory responses. Further understanding of how the inflammatory process works for animal species will be a determining factor in developing techniques to evaluate and potentially reduce inflammatory responses. Identifying markers that occur during the inflammatory states will provide a diagnostic tool for future therapeutic approaches.

Chapter 3: Objectives

The series objectives were:

Objective 1

To determine if protein profiles following *in vivo* LPS administration can be used as a biomarker. Genomics can give an insight into what may occur within a system, but protein-focused research can provide the ability to determine and measure activity as a function of time. Although proteomic-based research is inherently more complicated and more complex in comparison to genomics, proteins and their concentration levels remain a major factor in disease and normal physiology. To increase the understanding of the inflammation in a swine animal model, it is necessary to assess changes in expression patterns of plasma proteins after LPS administration. Utilizing and evaluating methodologies for protein detection is critical to biomarker discovery.

Objective 2

To examine the miRNA expression profiles for each LPS dosage level that can delineate between endotoxemia (or sepsis) and inflammation**.** The regulation of gene expression is a function of mature single-stranded miRNAs that are not translated into proteins but instead bound to messenger RNAs to purposely control translation and enhance mRNA degradation. To increase the understanding of post-transcriptional mRNA regulation, it is necessary to identify microRNAs that control gene expression

in inflammation and endotoxemia. There are several infection models that have been developed to reproduce aspects of inflammation based on the administration of a toxin, pathogen, or changes to the animal's endogenous protective barrier. The toxemia animal models have been commonly used to study the overall process of sepsis. Generally, circulating endotoxins in the subjects are required to meet the clinical definition of sepsis. The identification of unique miRNA biomarker signature(s) that can be detected is important to delineate between inflammation and sepsis. The role of these potential sepsis miRNA biomarkers could be used to determine if the subject is septic, the severity of the disease, and the ability to assess the response to treatment therapy.

Objective 3

To experimentally confirm if the swine miRNA-mRNA targets are as predicted in the human miRNA-mRNA target database. There are several online computational miRNA target prediction tool databases such as TargetScan and miRDB for species such as humans, mice, and rats. The limited computational and experimental information for swine, identifying the genes regulated by miRNAs has been a challenge. Focusing on the swine microRNAs of interest from the current study and utilizing the human miRNA prediction database, it can be determined if comparative analysis can be applied between species. The experimental results will provide insight

and supportive evidence into the biological function and targets of the swine miRNAs of interest post LPS-challenge.

Chapter 4: Proteomics evaluation of plasma to assess inflammation in swine

Abstract

In veterinary medicine, there has been an inability to assess inflammation in swine, due to a lack of qualified measures that can be used to evaluate the claims of drug efficacy. As a result, there are presently no approved therapies for controlling inflammation in this important food-producing animal. Therefore, the approval of drugs with anti-inflammatory claims in swine is impeded. The goal of this study was to evaluate changes in plasma proteins before and at time points following experimental induction by LPS. Comparison of protein expression patterns in control and LPS plasma samples collected from swine before and following challenge with *E. coli* were evaluated using one- and two-dimensional gel electrophoresis (1-DGE and 2-DGE). The comparison of plasma proteins over the course of inflammation was evaluated by nano-liquid chromatography coupled with tandem mass spectrometry (nLC-MS/MS). However, due to the complexity of the plasma samples, high-abundant plasma proteins presented limitations for assessing unique lower abundance protein biomarkers. Regardless of the total protein spots selected to be removed from each of the swine plasma 2-DGE gels, only twelve unique proteins were identified following nLC-MS/MS analysis of the peptides. The data presented provide added knowledge of potentially useful diagnostic markers of inflammation, including some new systemic indicators not previously considered.

Introduction

The detection of differentially expressed proteins in biological samples collected during altered physiological states has emerged as a promising approach to developing diagnostic indicators for companion and food animal disease. Recent efforts to detect modulated proteins in biological samples collected from animals, however, have shifted from traditional antibody-based approaches to large-scale chromatographic- and mass spectrometric-based proteomic analyses, due largely to the limited availability of species-specific antibodies (Jamie L. Boehmer, 2011; Lippolis & Reinhardt, 2010). To this end, the number of published reports of comparative proteomic studies performed using companion and livestock animal models has grown considerably in the past decade. Comparative studies in food animals have sought to define new indicators of disease or production traits of economic importance (Jamie L. Boehmer, 2011; Perez-Patiño et al., 2016).

The proteomics field has an established relationship between genes and diseases. Altered, missing, or defective proteins have been shown to be a cause of several diseases. Understanding protein interactions and pathways set the foundation for new drug therapy, discovery, and medicine. Currently, enzyme-linked immunosorbent assay (ELISA) is a quantification technique used to measure the presence of an antigen or an antibody in a sample. The limitation is that the technique only measures one protein. However, using proteomic techniques and quantification methodologies, it increases the threshold for the number of proteins that can be measured in a sample. Associating changes in protein expression with specific

diseases will lead to novel detection assays with high precision, accuracy, and reproducibility.

Protein biomarkers have been used for early detection and identification of cancer in humans using 2-DGE and surface-enhanced laser desorption ionization time-of-flight (SELDI-TOF) mass spectrometry. Applying technology and new methods, new protein biomarkers will lead to discovering the early stages of a disease (Wulfkuhle, Liotta, & Petricoin, 2003). Additionally, temporal expression changes of protein in milk after *E. coli* challenge have been identified in food animals such as bovine and goat using liquid chromatography, coupled with tandem mass spectrometry (LC-MS/MS). The ability to track relative protein abundance, detect low-abundance proteins and evaluate modified proteins in milk during the disease is a major advantage (Jamie L. Boehmer, 2011; J. L. Boehmer et al., 2010; Olumee-Shabon, Swain, Smith, Tall, & Boehmer, 2013). Recently, proteomic changes during inflammation at 24 and 48 hours by 2-DGE and nano-flow liquid chromatography (nLC) coupled to tandem mass spectrometry (MS/MS) were assessed in swine (Olumee-Shabon, Chattopadhaya, & Myers, 2020). The results of the study provide added information regarding the suitability and effectiveness of assessing swine plasma for proteomic analysis. In addition, the data offer insight into the temporal expression and changes in swine plasma proteins following experimental induction of *E. coli* lipopolysaccharide.

Materials and Methods

Pigs

Fifty-nine (59) Yorkshire swine barrows, weighing approximately 70kg, were used in the *in vivo E. coli* O55:B5 lipopolysaccharide (Sigma-Aldrich, St. Louis, MO) challenge. The pigs were given a healthy certificate. The Attending Veterinarian performed the health exam after at least one day of acclimation. The pigs had become familiar with daily human interaction which reduced physical restraint during sample collection and animal socialization. It was essential that the pigs were in safe and comfortable environment to achieve optimal physiological and psychological state for the animal's welfare. The Attending Veterinarian and the animal caretakers recorded abnormal health and behavior observations of each animal at time -24, -1, 0, and 1, 2, 3, 4, 6, 8, 24, and 48 hours post-LPS challenge. These clinical signs were used to determine if correlation between possible biomarkers and health observations can be established. The experimental protocol was approved by the Animal Care and Use Committee at the Office of Research, Center for Veterinary Medicine, U.S. Food and Drug Administration, and all procedures were conducted in accordance with the principles stated in the Guide for the Care and Use of Laboratory Animals (2010) and the Animal Welfare Act of 1966 (P.L. 89-544), as amended.

Escherichia Coli challenge

The *E. coli* O55:B5 lipopolysaccharide (LPS) technical grade was purchased from Sigma Chemical Company. The concentration of the LPS administered to the pigs was 1 mg/ml and the dosage, based on the success of previous studies, was 2 μg/kg (Peters et al., 2012). The swine that did not receive LPS received the same volumes and route of administration with sterile phosphate-buffered saline (PBS) as a negative control. The control with PBS and the LPS challenged group are the two treatment groups.

Blood collection

Each swine received an indwelling vascular catheter for blood collection which eliminates the use of mechanical restraints during the sampling process. Blood samples were collected at 0 hr (baseline), 1, 3, 8, and 24 hr post LPS challenge. 1 hr prior to the administration of LPS treatment, a baseline sample was collected. 20 ml of blood was centrifuged immediately for plasma extraction and used for assessing plasma proteins.

One-Dimensional Gel Electrophoresis (1-DGE) followed by in-gel digestion

Protein concentrations of swine plasma samples were determined using a bicinchoninic acid assay (Sigma-Aldrich; St. Louis, MO, USA) with bovine serum albumin (BSA) as the protein standard (Pierce; Rockford, IL, USA). The volume of each sample corresponding to 100 μg of total protein was made up to a final volume of 20 μL with water. The solution was mixed with an equal volume of Laemmeli

buffer (Bio-Rad Laboratories, Hercules, CA, USA) and 2 M dithiothreitol. The samples were heated to 65°C for 10 minutes. The samples were loaded on a 4-20% Tris-HCl polyacrylamide gels (Bio-Rad Laboratories, Hercules, CA, USA) in 1X Tris-glycine-SDS buffer at 200 V for 60 min. Gels were washed with deionized water (dH2O) for 5 mins, stained overnight in Coomassie Stain (Bio-Rad Laboratories, Hercules, CA, USA), and destained in dH2O for 1 hr at RT. Gels were imaged on a Molecular Dynamics personal densitometer SI (PDSI) image scanner (GE Healthcare BioSciences; Piscataway, NJ, USA). The optical densities of the gel lanes were determined by using the PDSI and TotalLab Quant software (TotalLab Ltd; Newcastle upon Tyne, NE1 2JE, UK).

The lanes were excised from the gel, cut into 12 slices, and destained at RT for 1 hr in 100 mM ammonium bicarbonate/50% acetonitrile for 15 min. It was repeated for 4 times or until the gel stains have been removed from the gel slices. Gel spots were dehydrated in 100% acetonitrile for 5 minutes at RT and dried to completeness in a vacuum centrifuge (GeneVac Inc.; Gardiner, NY, USA). 100 µL of 2 mM TCEP [tris(2-carboxyethyl)phosphine] in 25 mM ammonium bicarbonate was added to the dehydrated gel slices. The solution was placed in the incubator at 37 °C for 15 minutes and then the supernatant was discarded. 100 µL of 20 mM iodoacetamide in 2 5mM ammonium bicarbonate was added to the gel pieces. The solution was placed in the incubator at 37 °C for 15 minutes and then the supernatant was discarded. The gel slices were washed three times with 200 µL of 25 mM ammonium bicarbonate for 15 min each. Gel spots were dried to completeness in a vacuum centrifuge (GeneVac

Inc.; Gardiner, NY, USA). Slices were rehydrated in 0.4 µg of sequence-grade modified trypsin (Promega Corporation; Madison, WI, USA) in 40 mM ammonium bicarbonate, and allowed to digest for 16 hr at 37 °C. After digestion the solution was transferred to a clean micro centrifuge tube. The peptides in the gel were extracted with 50% acetonitrile/5% formic acid at RT for 1 hr. The extracted peptides and the solution from the overnight digestion were pooled. The combined solution was concentrated in a vacuum centrifuge (GeneVac Inc.; Gardiner, NY, USA) for 20 mins at 22 °C. Extracted peptides were stored at -20 °C until analysis.

Two-Dimensional Gel Electrophoresis (2-DGE) followed by in-gel digestion

Protein concentrations of plasma samples were determined using a bicinchoninic acid assay (Sigma-Aldrich; St. Louis, MO, USA) with bovine serum albumin (BSA) as the protein standard (Pierce; Rockford, IL, USA). The volume of each sample corresponding to 150 µg was combined with rehydration buffer (8 M urea, 2% 3-[(3-cholamidopropul) dimethylammonio]-1-propanesulfonate, 50mM dithiothreitol, 0.2% BioLyte 3/10 ampholyte, 0.001% Bromophenol Blue; Bio-Rad Laboratories, Hercules, CA, USA) to a final volume of 150 µL, and applied to an 11-cm pH 3-10 nonlinear immobilized pH gradient (IPG) strips (Bio-Rad Laboratories, Hercules, CA, USA). The strips were covered with mineral oil, and incubated overnight at RT. The IPG strips were focused in a Bio-Rad Protean IEF cell (Bio-Rad Laboratories, Hercules, CA, USA) for 20 hrs using the following voltage intervals: 500 V for 1 hr, 1,000 V for 1 hr, 2,000 V for 2 hr, 4,000 V for 4 hr, and 8,000 V for 12 hr. The IPG strips were reduced

in equilibration buffer I (6 M urea, 2% SDS, 0.375 M Tris-HCl pH 8.8, 20% glycerol; Bio-Rad Laboratories, Hercules, CA, USA), with 2% dithiothreitol (DTT; wt/vol) at RT for 15 min. Following reduction, the IPG strips were alkylated in equilibration buffer II (6 M urea, 2% SDS, 0.375 M Tris-HCl pH 8.8, 20% glycerol; Bio-Rad Laboratories, Hercules, CA, USA) with 2.5% (wt/vol) iodoacetamide at RT for 15 min. The IPG strips were run in the second dimension on 10-20% Tris-HCl polyacrylamide gels (Bio-Rad Laboratories, Hercules, CA, USA) in 1X Tris-glycine-SDS buffer at 200 V for 60 min. Gels were washed with dH2O for 5 mins, stained overnight in Coomassie Stain (Bio-Rad Laboratories, Hercules, CA, USA), and destained in dH2O for 1 hr at RT. Gels were imaged on a Molecular Dynamics personal densitometer SI (PDSI) image scanner (GE Healthcare BioSciences; Piscataway, NJ, USA).

Protein spots were excised from 2-D gels with either a 1.5 mm or 3.0 mm OneTouch 2-D gel spot picker (Gel Company; San Francisco, CA, USA). Identical spots of interest present in each gel were excised and destained at RT for 1 hr in 50 mM ammonium bicarbonate/50% acetonitrile. Gel spots were dehydrated in 100% acetonitrile for 5 minutes at RT and dried to completeness in a vacuum centrifuge (GeneVac Inc.; Gardiner, NY, USA). Spots were rehydrated in 0.4 µg of sequence-grade modified trypsin (Promega Corporation; Madison, WI, USA) in 40 mM ammonium bicarbonate, and allowed to digest for 16 hrs at 37 °C. After digestion, the solution was transferred to a clean microcentrifuge tube. The peptides in the gel were extracted with 50% acetonitrile/5% formic acid at RT for 1 hr. The extracted peptides and the solution from the overnight digestion were pooled. The combined solution was

concentrated in a vacuum centrifuge (GeneVac Inc.; Gardiner, NY, USA) for 20 mins at 22 °C. Extracted peptides were stored at -20 °C until analysis.

In-solution digests

A volume of each plasma fraction corresponding to 1 mg of total protein was diluted in 100 mM ammonium bicarbonate buffer to a final volume of 15 0µL, and reduced in a final concentration of 5 mM tris(2-carboxyethyl)phosphine (TCEP; Promega; Madison, WI, USA) for 30 minutes at RT. Samples were alkylated in a final concentration of 10 mM iodoacetamide for 30 minutes at RT in the dark. Approximately 5 µg of sequencing grade modified trypsin (Promega) was added to each sample to achieve a 1:200 enzyme-to-protein ratio, and digestion was carried out for 16 hrs at 37 °C. The digestions were quenched by the addition of acetic acid to a final concentration of 0.1% and stored at -20 °C until further analysis.

Chromatography and mass spectrometry

Prior to analysis, each in-solution digest was diluted 1:100 (digest: diluent) in 0.1% formic acid. One-dimensional LC-MS/MS analyses were carried out by injecting 5 µL of either each undiluted in-gel digest or each diluted in-solution plasma digest into a nanoflow high-performance LC (HPLC) instrument (Eksigent; Dublin, CA, USA), coupled to a linear ion trap LTQ Velos mass spectrometer (Thermo Fisher Scientific; Waltham, MA, USA). Peptides were loaded onto a nanoAcquity 100µm x 100mm C18 reverse phase UPLC column (Waters; Milford, MA, USA). The mobile phases consisted of 0.1% formic acid in water (A) and 0.1% formic acid in acetonitrile (B).

For in-gel digests, peptides were eluted with the following gradient: 5-20% B in 15 min, 20-60% B in 10 min, 60-80% B in 5 min, and 80-95% B in 5 min at a flow rate of 500 nl/min. For in-solution digests, peptides were eluted with the following gradient: 5-20% B in 25 min, 20-60% B in 25 min, 60-80% B in 20 min, and 80-95% B in 5 min at a flow rate of 500 nl/min. All eluates were electrosprayed by applying 1.6 kV to the terminal PicoTip emitter (25 µm i.d., 30 µm i.d. tip; New Objective; Woburn, MA, USA). The LTQ Velos mass spectrometer was operated in positive ion mode, and spectra were acquired for 50 min for in-gel digested samples and 70 min for in-solution digested samples in data-dependent tandem MS mode. The six most intense ions in each MS survey scan (over the range 400 to 2000 m/z) were subjected to MS/MS by collision-induced dissociation (CID) for in-gel digested samples. The ten most intense ions in each MS survey scan (over the range 400 to 2000 m/z) were subjected to MS/MS by CID for in-solution digested samples. The normalized collision energy used to fragment each peptide ion was 35%. Following MS/MS, precursor ions were excluded from MS/MS analysis for 45 sec. Mass spectral peak lists were generated using Proteome Discoverer software (Thermo Fisher Scientific; Waltham, MA, USA) without smoothing or signal-to-noise thresholding. All samples were analyzed in duplicate.

Informatics

Mass spectral peak lists were submitted to the Mascot search engine (v. 2.3.0; Matrix Sciences; London, UK) using Proteome Discover (v1.2; Thermo Scientific, Waltham, MA, USA) and searched against the UniprotKB Swiss-Prot protein sequence library (v.57.15; http://www.uniprot.org). The following search parameters were applied: *other mammalia* species, trypsin enzyme, three allowed missed cleavages, carbamidomethylation static modification, methionine oxidation dynamic modification, precursor ion mass tolerance of ± 1.3 Da, and a fragment ion mass tolerance of ± 0.8 Da. The number of sequences searched in the *other mammalia* taxonomy was 64,838. All data were filtered by peptide Ion Score greater than the Mascot Identity Threshold (at $P < 0.05$), number of peptides per protein ($n \geq 2$), and by number of spectral counts per protein (≥ 4). Temporal expression of individual proteins was determined using normalized spectra counts, which is the total number of MS/MS spectra assigned to peptides by Mascot. Normalization of spectral counts was performed as previously described (Jamie L. Boehmer, 2011; McFarland, Ellis, Markey, & Nussbaum, 2008). Briefly, for each biological replicate, the total spectral counts for a given protein (pooled technical replicates) was divided by the sum of all spectral counts for all proteins (pooled technical and biological replicates) identified at each given time point.

Results

Comparison of 1-DGE profiles of un-depleted swine plasma samples

Initially, the temporal expression of each treatment group was represented in a one-dimensional gel prior to protein identification by nano-LC-MS/MS analysis (Figure 1A-B). Coomassie dye combined with gel electrophoresis allows for staining and the visualization of the broadest spectrum of proteins. First, using the bicinchoninic acid assay technique, the protein concentrations of all the swine plasma samples were measured and recorded (Table 1). The total volume of each band slice on the gels was calculated using a PDSI image scanner and the TotalLab Quant image analysis software. The intensity peaks of each gel slice from a control and LPS treated swine were analyzed and normalized to a standard intensity from a marker standard on their respective gels (Figure 2A-B). Bands displaying different intensity or unique were measured and compared between animal treatment groups. Analyzing the intensity trends in the bands during the time course was a preliminary step in associating changes and determining the approximate molecular weight sizes for those proteins. The highest intensity for all bands, except for band number 5, for the LPS group was at the 3 hour timepoint (Figure 2B). This is an indication that the highest degree of protein up-regulation due to solely LPS infection would be possibly recognized in the 3 hour sample sets. The majority of the LPS group bands trend downward towards the baseline values between 8 and 24 hr. Selected bands of interest were sliced into 1mm pieces for further nLC-MS/MS analyses (Table 2). The detection and identification of

swine proteins found in at least four time points were assessed in the LPS treatment groups (Table 1). Alpha-1-antitrypsin (A1AT), Alpha-2-HS-glycoprotein (FETUA), C-reactive protein (CRP), Haptoglobin (HPT), Serum amyloid P-component (SAMP), Complement component C7 (CO7), and Von Willebrand factor (VWF) were the positive acute phase proteins present in the LPS group over time Table 2. The negative acute phase proteins Serotransferrin (TRFE), Serum albumin (ALBU), and Transthyretin (TTHY) were also found (Table 2). These acute phase proteins are known indications for the innate immune system (Jain, Gautam, & Naseem, 2011).

Table 1. Protein Concentration of Swine Plasma

Protein Concentration determined by Bicinchoninic Acid Assay.

Control swine plasma samples (ng/ul)					
Pig Number[1]	**0hr**	**1hr**	**3hr**	**8hr**	**24hr**
6	63.28	69.42	66.41	61.61	70.53
8	61.08	63.59	62.24	81.55	73.16
11	62.46	61.34	58.26	54.50	64.02
19	59.68	65.44	77.81	55.98	59.21
22	64.22	66.88	68.59	46.27	62.78
40	61.00	65.21	66.01	63.97	55.16
46	65.44	68.94	57.17	67.88	49.68
35	66.72	57.52	54.03	56.82	49.45
42	71.26	57.79	74.49	105.87	59.36
LPS swine plasma samples (ng/ul)					
2	63.85	45.11	47.11	59.57	58.44
7	64.44	67.04	50.44	39.32	94.84
10	66.43	72.34	53.23	N/A	N/A
13	52.64	61.78	61.79	53.19	61.93
32	46.08	56.53	58.94	67.48	52.61
43	47.70	53.96	54.39	60.65	55.57
45	58.01	74.77	68.17	57.03	65.10
34	59.23	47.96	56.71	50.14	59.69
41	64.31	53.58	48.95	57.99	48.53

1 = Number corresponds to ear tag number used for identification

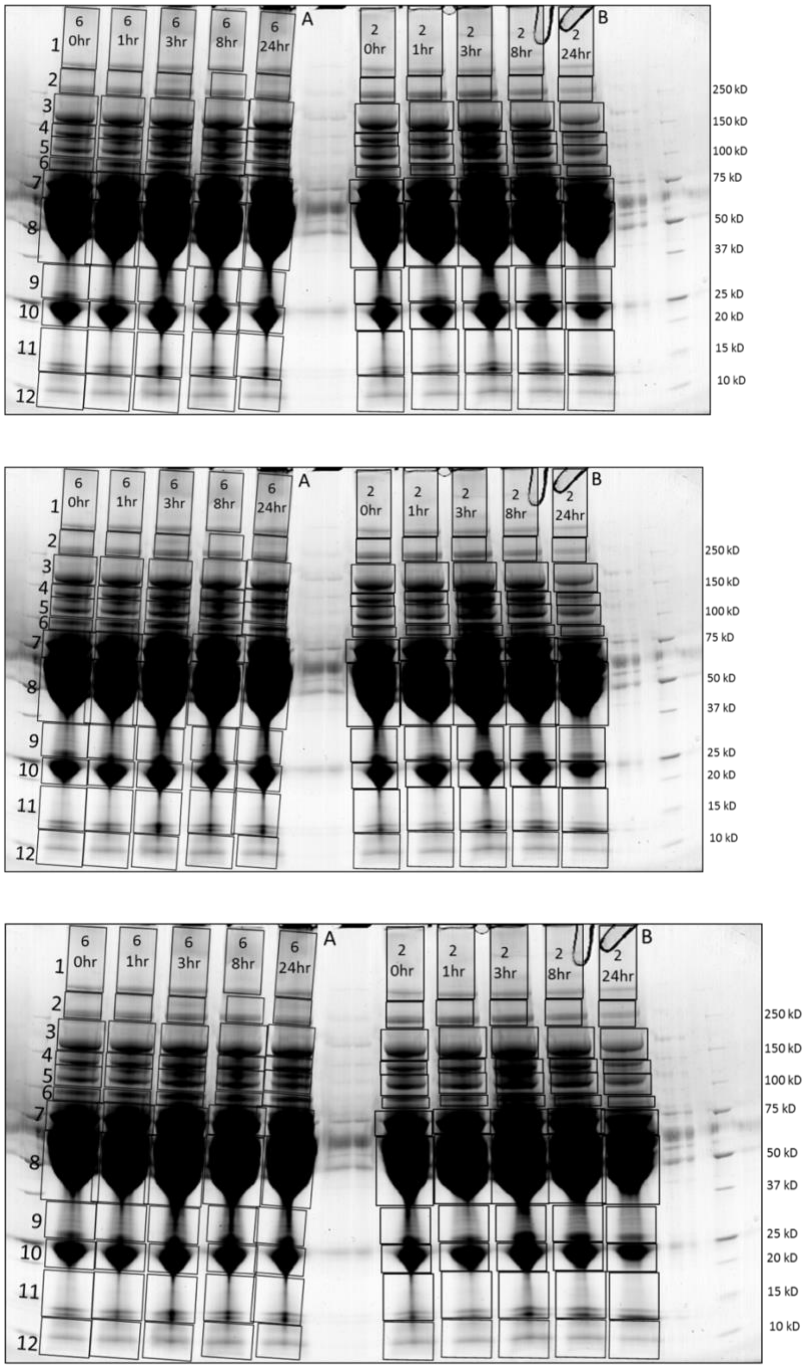

Figure 1. One-dimensional gel profiles. Representative one-dimensional gel profiles of swine plasma collected at 0 hr, 1 hr, 3 hr, 8 hr, and 24 hr for the control group (A) and following LPS challenge (B).

A

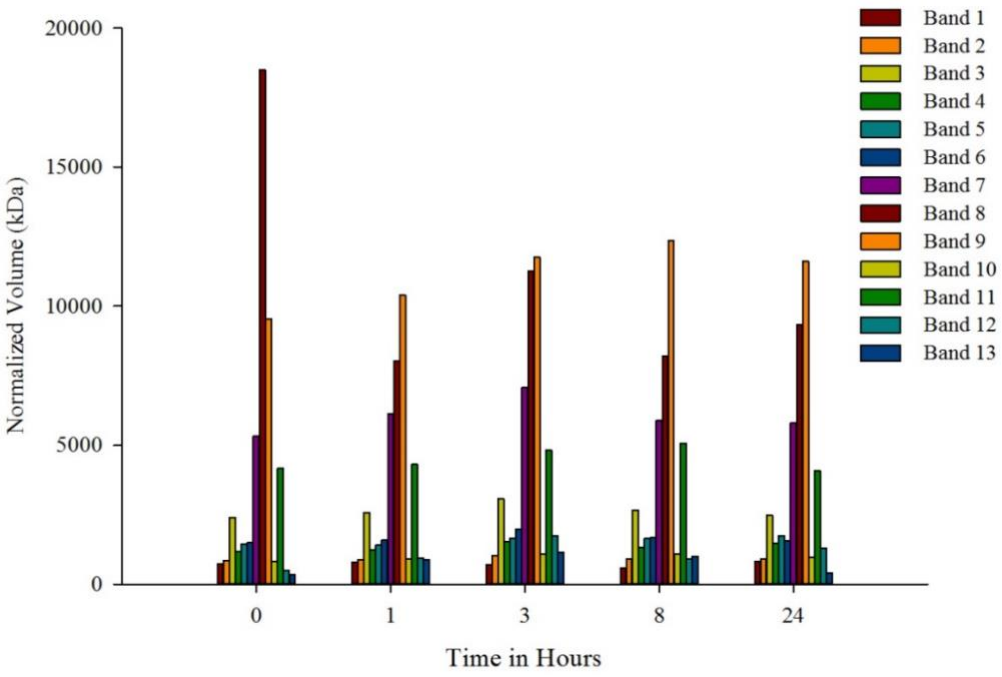

B

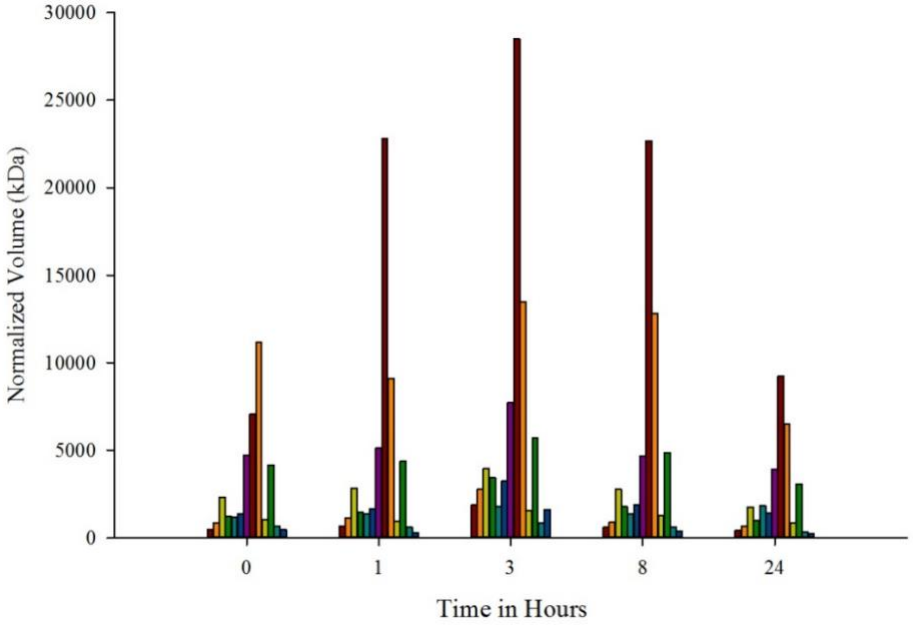

Figure 2. Band intensity analysis of one-dimensional gels. Representative time course of the normalized volumes (kDA) of the 1D swine plasma of the control (A) and LPS induced swine (B). Band numbers correspond to bands excised from the numbered bands in (Figure 1).

Table 2. One-DGE Swine Proteins

Swine plasma proteins detected following the LC-MS/MS of 1-DGE band digestion of LPS treatment

Swiss-Prot Entry Name	Accession Number	Protein Name	Time Point Detected (hr)	Biological Function
A1AT	P50447	Alpha-1-antitrypsin	0, 1, 3, 8, 24	Inhibitor of serine proteases.
FETUA	P29700	Alpha-2-HS-glycoprotein	0, 1, 3, 8, 24	Plasma glycoprotein.
APOA1	P18648	Apolipoprotein A-I	0, 1, 3, 8, 24	Transport protein; major plasma HDL protein.
APOA4	O46409	Apolipoprotein A-IV	0, 3, 8, 24	Role in chylomicrons and VLDL secretion and catabolism.
APOE	P18650	Apolipoprotein E	0, 1, 3, 8, 24	Mediates the binding, internalization, and catabolism of lipoprotein particles.
CLUS	Q29549	Clusterin	0, 1, 3, 8, 24	Functions as extracellular chaperone that prevents aggregation of nonnative proteins.
CO7	Q9TUQ3	Complement component C7	0, 1, 3, 8	A membrane anchor that plays a key role in the innate and adaptive immune response.
CRP	O19062	C-reactive protein	0, 3, 8, 24	Associated with host defense and may scavenge nuclear material released from damaged circulating cells.
GELS	P20305	Gelsolin (Fragments)	0, 1, 3, 8, 24	Actin-modulating protein that binds to the plus ends of actin monomers, preventing monomer exchange.
HPT	Q8SPS7	Haptoglobin	0, 3, 8, 24	Captures, and combines with free plasma hemoglobin to allow hepatic recycling of heme iron.
HBA	P01965	Hemoglobin subunit alpha	0, 3, 8, 24	Involved in oxygen transport from the lung to the various peripheral tissues.
HBB	P02067	Hemoglobin subunit beta	0, 3, 8, 24	Involved in oxygen transport from the lung to the various peripheral tissues.
HEMO	P50828	Hemopexin	0, 3, 8, 24	Binds heme and transports it to the liver for breakdown and iron recovery.
LAC	P01846	Ig lambda chain C region	0, 1, 3, 8, 24	Chain obtained from a mixture of normal immunoglobulins.
ICA	Q29545	Inhibitor of carbonic anhydrase	0, 1, 3, 8	Inhibitor for carbonic anhydrase 2 (CA2). Does not bind iron ions.
ITIH1	Q29052	Inter-alpha-trypsin inhibitor heavy chain H1	0, 1, 3, 8, 24	May act as a carrier of hyaluronan in serum /or as a binding protein between hyaluronan and other matrix protein.
ITIH2	O02668	Inter-alpha-trypsin inhibitor heavy chain H2	0, 1, 3, 8, 24	May act as a carrier of hyaluronan in serum or as a binding protein between hyaluronan and other matrix protein.
ITIH4	P79263	Inter-alpha-trypsin inhibitor heavy chain H4	0, 1, 3, 8, 24	May be involved in acute phase reactions
PLMN	P06867	Plasminogen	0, 1, 3, 8, 24	Dissolves the fibrin of blood clots and acts as a proteolytic factor in inflammation.
THRB	Q19AZ8	Prothrombin	0, 1, 3, 8, 24	Functions in blood homeostasis, inflammation and wound healing
TRFE	P09571	Serotransferrin	0, 1, 3, 8, 24	Transport of iron from sites of absorption and heme degradation to those of storage and utilization.

ALBU	P08835	Serum albumin	0, 1, 3, 8, 24	The function is the regulation of the colloidal osmotic pressure of blood.
SAMP	O19063	Serum amyloid P-component	0, 1, 3, 8, 24	Cofactor that binds 2 calcium ions per subunit.
TTHY	P50390	Transthyretin	0, 3, 8, 24	Thyroid hormone-binding protein. Probably transports thyroxine from the bloodstream to the brain
TRYP	P00761	Trypsin	0, 1, 3, 8, 24	Proteolytic enzyme and involved in the digestion of proteins.
VWF	Q28833	Von Willebrand factor (Fragment)	0, 1, 3, 8, 24	Maintenance of hemostasis by promoting adhesion of platelets to the sites of vascular injury

Comparison of 2-DGE profiles of swine plasma samples

Two-dimensional-GE profiles of plasma collected from control and LPS treatment groups at 0 hr (baseline) and 1 hr were generated to perform a preliminary analysis of changes in the swine plasma proteome as a result of LPS induction (Figure 3A-D). The sequencing of tryptic peptides using nLC-MS/MS was the technique used for the identification of proteins in each of the different proteomic approaches. All spectra data was searched against the SwissProt database using MASCOT with strict search criteria for protein identification. Samples collected at 3, 6, 12, and 24 hr marks following infection were not included in these experiments, as preliminary 2-DGE analyses revealed comparable protein expression patterns. Largely, the same proteins were detected on the 2-DGE gels of the baseline and 1 hr control plasma samples; however visually some of the spots corresponding to spots 1-3, 5, 8, 13, 16, 23, 24, 33, 25, 30-37, 39, 40, 41 were present in either the baseline and 1 hr control (Figure 3A-B) and not the 1 hr LPS samples (Figure 3D). Although definitive spot identifications were not confirmed due to the filter criteria, deductive evaluations were considered for same number gel spots in different time points within treatment

groups. An increased intensity of alpha-2-HS-glycoprotein (spot 7) appears from baseline to 1 hr in the control group (Figure 3A-B). A visual inspection of the protein profiles suggested a decrease intensity in spots corresponding to clusterin (spot 7) from 0 to 1 hr following infection (Figure 3C-D). Additionally, the plasminogen (spot 34) intensity appears to decrease from 0 to 1 hr in both control and LPS treatment group. However in the 1 hr LPS gel, the spot is non-detectable (Figure 3D). A larger number of protein spots were excised from gels than the number of proteins reported. However, some proteins were exempted from the set of data because peptide identifications did not meet the inclusion criteria. The criteria ensured that positive protein identification from the Mascot database was accurate, sensitive, and specific from the analyzed peptides. Regardless of the 41 protein spots selected and removed from each of the swine plasma 2-DGE gels, only eleven unique proteins were identified following nLC-MS/MS analysis of the peptides: alpha-2-HS-glycoprotein, clusterin, hemoglobin, Ig lambda chain, Keratin (type I and II), plasminogen, serotransferrin, serum albumin, Thioredoxin, and trypsin (Table 3 and 4). The limited data for protein changes across time and groups created a challenge for analysis. Although visual changes were observed in the gels, due to the inclusion criteria which led to unfavorable results for the changes in proteins of interest, alternative methods such as in-solution digestion and quantitative real-time-PCR were considered for biomarker discovery.

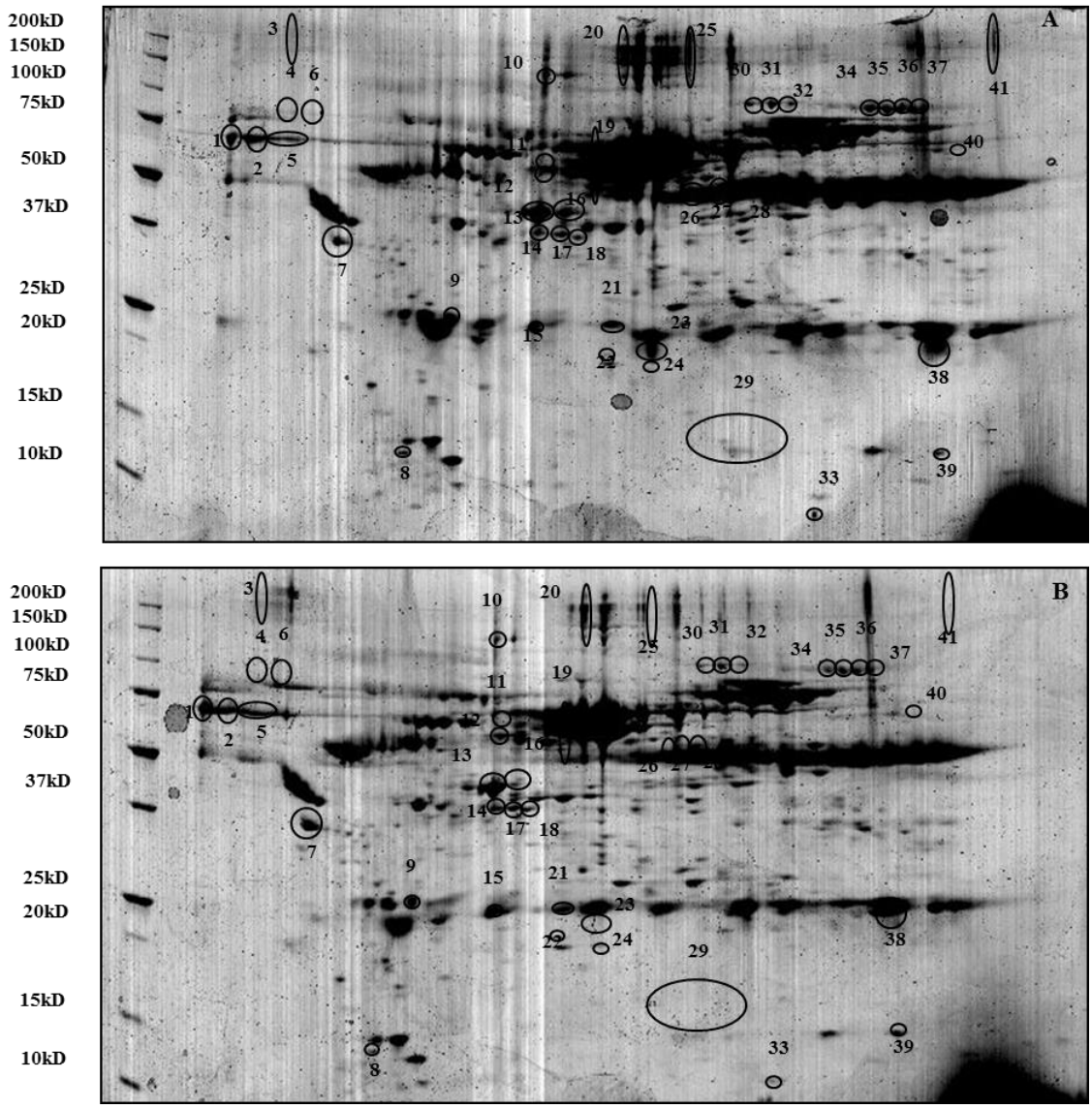
200kD
150kD
100kD
75kD
50kD
37kD
25kD
20kD
15kD
10kD
A
B

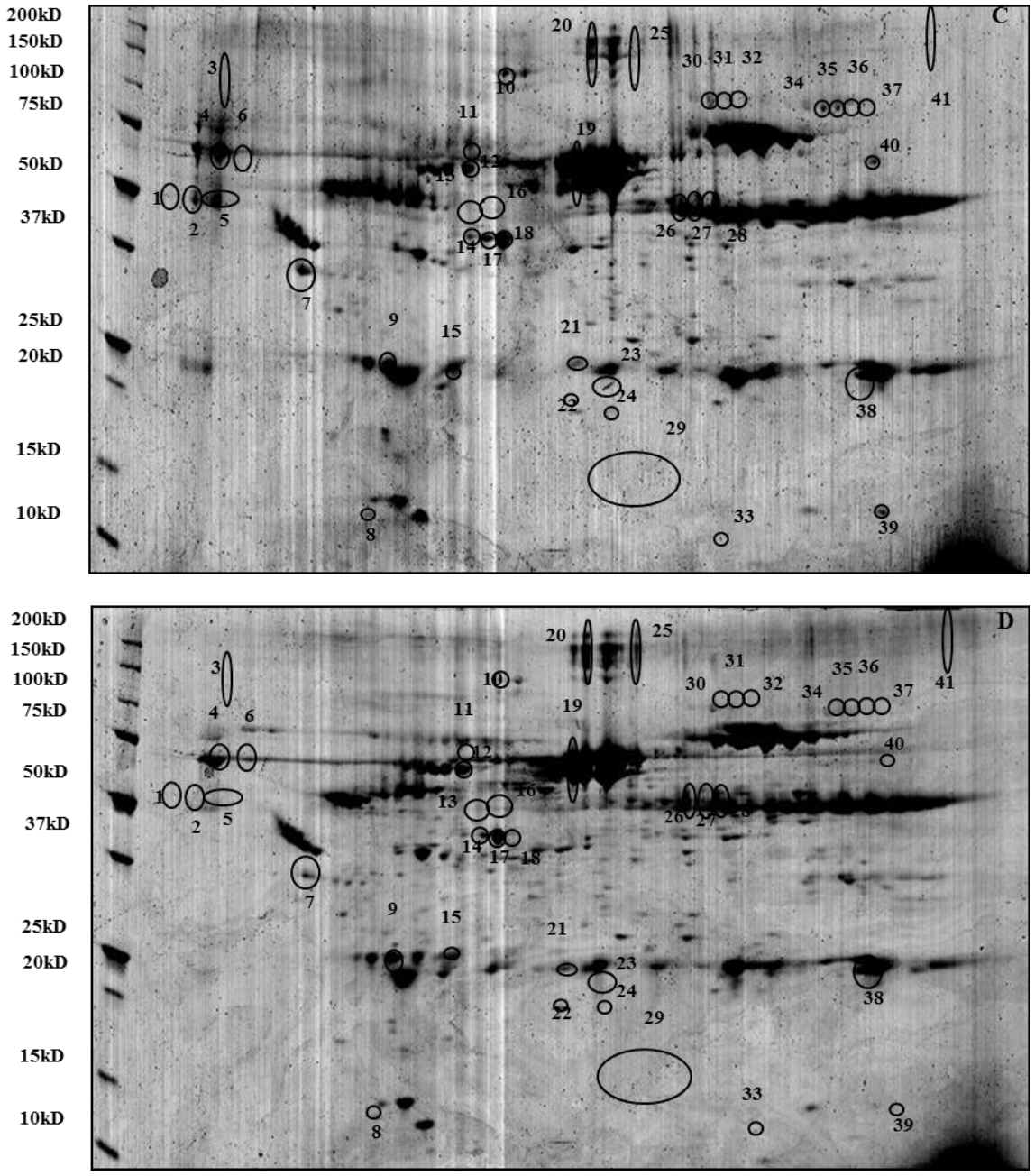

Figure 3. Two-dimensional gel profiles. Representative two-dimensional gel profiles of the control swine plasma at 0 hr (A), at 1 hr (B), LPS induced swine collected prior to infection with *E. coli* (C), and at 1 hr (D) following infection. Spot numbers correspond to those in Table 3. Proteins in 2-DGE Control Group at 0 and 1 hr (Table 3 and 4).

Table 3. Proteins in 2-DGE Control Group at 0 and 1 hr

Proteins detected in 2-DGE of baseline swine plasma

Spot Number[1]	Swiss-Prot Entry Name	Protein Name	Accession Number	Peptides[2]	% Coverage[3]
1	TRYP	Trypsin	P00761	2.0	12.99
2, 16, 40	ALBU	Serum albumin	P02769	2.0	3.84
34	PLMN	Plasminogen	P06867	1.0	3.46
39	HBB	Hemoglobin	B3EWC8	2.0	15.75
3, 4, 5, 6, 7, 8, 9, 10, 11, 12, 14, 15, 17, 18, 19, 20, 21, 22, 23, 24, 25, 26, 27, 28, 29, 30, 31, 32, 33, 35, 36, 37, 38, 41	No Data	N/A	N/A	N/A	N/A

Proteins detected in 2-DGE of 1 hr swine plasma

Spot Number[1]	Swiss-Prot Entry Name	Protein Name	Accession Number	Peptides[2]	% Coverage[3]
1, 5, 10	ALBU	Serum albumin	P02769	3.0	8.87
7	FETUA	Alpha-2-HS-glycoprotein	P12763	2.0	9.12
2, 3, 4, 6, 8, 9, 11, 12, 13, 14, 15, 16, 17, 18, 19, 20, 21, 22, 23, 24, 25, 26, 27, 28, 29, 30, 31, 32, 33, 34, 35, 36, 37, 38, 39, 40, 41	No Data	N/A	N/A	N/A	N/A

1 = Number corresponds to spot number on gel in Figure 3A-B
2 = Number represents peptides assignments (peptide assignments were averaged if protein was detected in more than one spot on a gel).
3 = Percent coverage of protein based on peptide assignments or average percent coverage if protein detected in more than one spot.

Table 4. Proteins in 2-DGE LPS Group at 0 and 1 hr

Proteins detected in 2-DGE of 0 hr swine plasma following infection with *E. coli*

Spot Number[1]	Swiss-Prot Entry Name	Protein Name	Accession Number	Peptides[2]	% Coverage[3]
4, 17, 26, 30, 31, 36	K1C10	Keratin, type I	Q6EIZ0	2.17	6.68
6, 9, 11, 14, 15, 24, 34, 35	K2C6A	Keratin, type II	P02538	2.75	5.11
7	CLUS	Clusterin	Q29549	2.00	5.83
12	TRFE	Serotransferrin	Q29443	4.00	8.33
18, 19, 28	ALBU	Serum albumin	P02769	3.33	7.25
37	PLMN	Plasminogen	P06867	2.00	3.46
1, 2, 3, 5, 8, 10, 13, 16, 22, 23, 25, 27, 29, 32, 33, 38, 39, 40, 41	No Data	N/A	N/A	N/A	N/A

Proteins detected in 2-DGE of 1 hr swine plasma following infection with *E. coli*

Spot Number[1]	Swiss-Prot Entry Name	Protein Name	Accession Number	Peptides[2]	% Coverage[3]
3	THIO	Thioredoxin	P0AA27	2.0	28.44
9	LAC	Ig lambda chain C	P01846	3.0	35.24
1, 2, 4, 5, 6, 7, 8, 10, 11, 12, 13, 14, 15, 16, 17, 18, 19, 20, 21, 22, 23, 24, 25, 26, 27, 28, 29, 30, 31, 32, 33, 34, 35, 36, 37, 38, 39, 40, 41	No Data	N/A	N/A	N/A	N/A

1 = Number corresponds to spot number on gel in Figure 3C-D
2 = Number represents peptides assignments (peptide assignments were averaged if protein was detected in more than one spot on a gel).
3 = Percent coverage of protein based on peptide assignments or average percent coverage if protein detected in more than one spot.

In-solution digestion of swine plasma

In-solution digestion followed by nLC-MS/MS with label-free quantification was performed to evaluate trends and increasing protein sequence coverage. Only the following six proteins met the criteria that the protein should be present in each sample and detectable throughout the entire time course: alpha-2-HS-glycoprotein, apolipoprotein A-1 (APOA1), haptoglobin (HP), hemopexin, serotransferrin, and serum albumin. Expectedly, the largest change occurred at 24 hr with the LPS treatment groups of swine. Acute phase proteins have been shown to reach their peak

24 to 48 hrs as an inflammatory response. Apolipoprotein A-1 (Figure 4A) and haptoglobin (Figure 4B) exhibited down and up regulation for the LPS group at the 24 hr time point, respectively. The temporal expression of haptoglobin appeared to be inverted with respect to LPS and control treatment group (Figure 4B). These results show how the abundance and regulation of haptoglobin in plasma is essential to characterizing diseased and healthy swine. Although serum albumin has been known to be a negative acute-phase protein (APP) during inflammatory state, during this time course in swine it appears to remain relatively stable within all groups (Figure 4C). The apparent decrease that serum albumin has exhibited as a negative APP may not actually be a decrease in production but the relative increase expression of other serum APP. Serum APPs outside of serum albumin may be attributed to and responsible for the measured albumin present and its concentration cannot be directly attributed to a change in production.

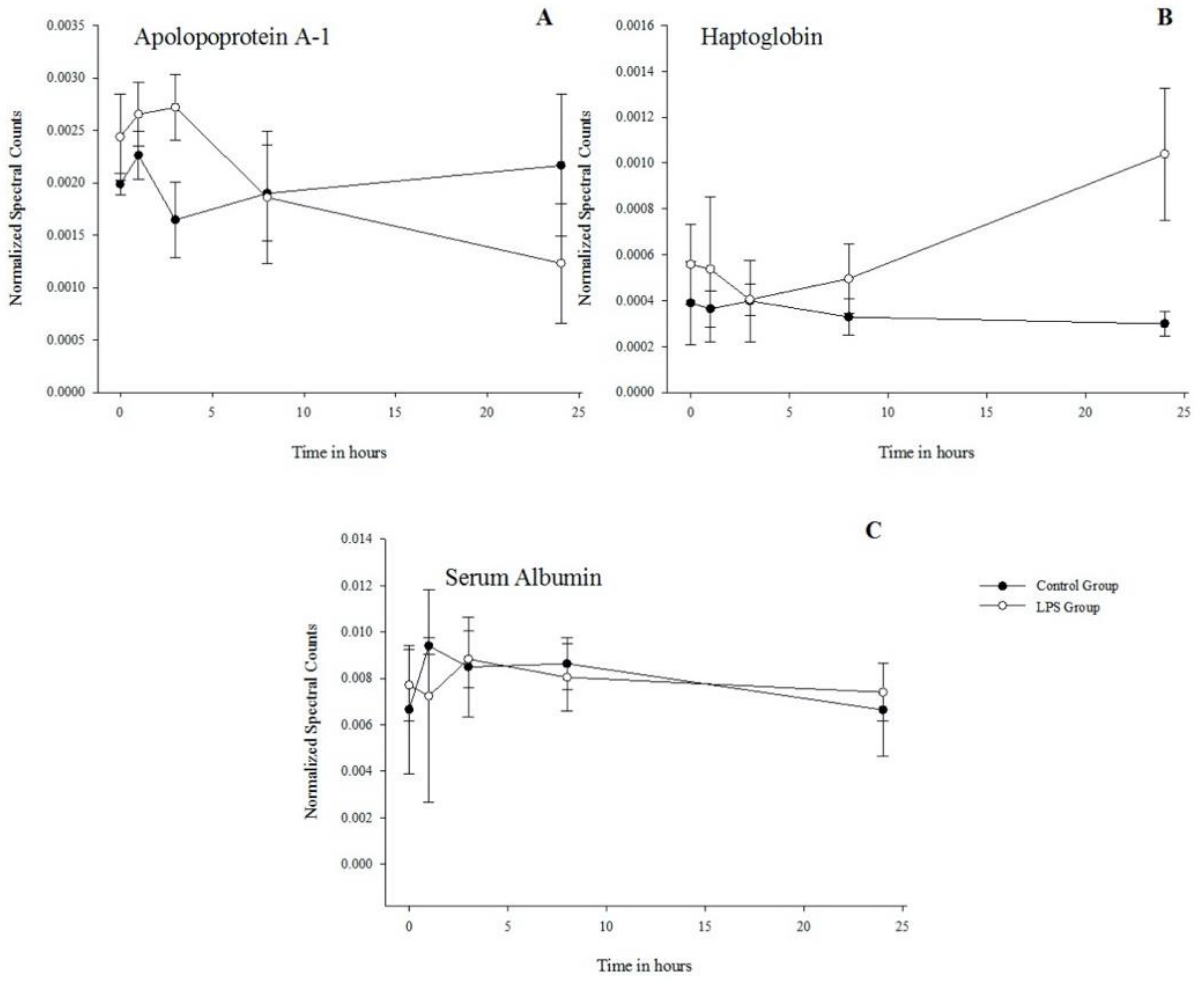

Figure 4. In-solution protein expression levels. Control and LPS plots at 0, 1, 3, 8, and 24 hr of protein expression levels. Temporal expression patterns (mean spectral counts ± standard error) of the proteins apolipoprotein A-1 (A), haptoglobin (B) and serum albumin (C) in solution digestion fractions.

Discussion

Proteomic strategies were used to assess potential changes in the swine plasma proteome as a result of the experimental induction of LPS. The aim of this study was to explore protein biomarkers with significant differential expressions that

have not been previously associated with inflammation in swine. The current study examined expression patterns of selected proteins in plasma samples from non-LPS treated control swine, compared with those swine dosed with LPS over time. Using an *in vivo* swine model system, we demonstrated the involvement of several proteins in systemic inflammatory responses.

Initial investigation used 1-DGE to visualize and calculate the intensity of the peaks for their respective gels. In gel digestion of the band slices were profiled by 1-DGE and proteins of interest were excised from gels, digested with trypsin, and the resulting tryptic peptides were sequenced using 1-dimensional nLC-MS/MS. The swine proteins that were presented during the majority of the LPS time course were of high interest. Based on previous findings, it was understandable that APPs were present in this inflammation study. The present positive APPs detected in the 1-DGE, such as CRP, HPT, SAMP, CO7, and VWR may destroy or hinder the growth of microbes while the negative APPs such as TRFE, ALBU and TTHY decrease during inflammation (Charlie-Silva et al., 2019).

Further assessments of modulation of the swine plasma proteome during *E. coli* mastitis were performed using nLC-MS/MS of in-solution digested plasma samples collected for control group and LPS induced group at 0, 1, 3, 8, and 24 hour marks. Normalized values for spectral counts assigned to the proteins detected were used as a means to assess temporal expression of a select number of swine plasma proteins detected in swine plasma before and following the induction of LPS including APPs, abundant plasma proteins, and the apolipoproteins. In inflammation,

acute phase proteins produced in the liver are known to increase concentration by 25% in the plasma (Gabay & Kushner, 1999). Although previous swine studies have shown an increase in haptoglobin up to 8-fold in 48 to 72 hr after inducing inflammation, the increase shown at 24 hr demonstrates similar trends (Lampreave et al., 1994). It has recently been demonstrated that serum albumin protein modulation from inflammation at 24 hr may be related to the changes observed with this study (Olumee-Shabon et al., 2020). APPs remain a prominent focus in veterinary biomarker disease research due largely to their suspected potential to serve as reliable diagnostic indicators of inflammation and disease.

Veterinary biomarker studies continue to suffer from an inadequate number of biological replicates, the lack of a uniform proteomic approach to sample analysis, and insufficient statistical models for accurate data analysis. However, each separate analysis provides additional data and insight. The results of the current analyses provide, independent of the need for antibody development, preliminary data on the timeframe in which certain APPs and proteins related to the host response peak in abundance in swine plasma following *E. coli* infection. This study was intended to determine changes in proteins in the early timepoints to compare each treatment group. However, the lack of significant differences between 1 and 3 hr between the groups resulted in seeking alternative biomarkers. Cumulatively, the data presented provide added knowledge of potentially useful diagnostic markers of swine inflammation, including some new systemic indicators not previously considered.

Chapter 5: Lipopolysaccharide (LPS) induced inflammatory changes in miRNA expression correlates to the severity of the host inflammatory response

Abstract

In veterinary medicine, inflammation in swine is evaluated principally by clinical signs. This method is often unreliable when assessing large animal populations because of inconsistent interpretations of clinical observations. This study examined whether changes in miRNA expression can predict the severity of the inflammatory response in swine after administration of Escherichia coli lipopolysaccharide (LPS). Whole blood from swine challenged with LPS at 0.125 µg/kg to 2.0 µg/kg body weight was collected at 0, 1, 3, 8, and 24 hrs post LPS-challenge. Mature miRNAs were extracted from plasma and quantitative real-time-PCR (qRT-PCR) was used to evaluate the 84 most abundant swine miRNAs found in plasma. The miRNA changes in expression were assessed using the comparative CT Method (ΔΔCT method) for normalization with an exogenous control. The results revealed that expression of ssc-let-7e-5p, ssc-mir-22-3p, and ssc-miR-146a-5p were the most significantly changed miRNA over the time course. At 1 hr post-LPS, ssc-let-7e-5p decreased as the LPS dosage levels increased from 0.125 to 1.0 µg/kg. Similarly, as the LPS doses increased from 0.125 to 0.5 µg/kg, ssc-miR-22-3p levels significantly decreased at 1 hr post-LPS. In the 2.0 µg/kg LPS, ssc-miR-146a-5p levels increased between 0 and 3

hrs post-LPS; however, expression was downregulated with a 145% decrease from 3 to 8 hrs. The three miRNA biomarkers suggest potentially useful surrogate endpoints for the evaluation of inflammatory and endotoxemia responses in swine.

Introduction

In veterinary medicine, it has been difficult to evaluate the capacity for drugs to control inflammation in swine due to a lack of qualified measures that can be used to substantiate the drug claims. Currently, inflammation in swine is evaluated principally by clinical signs, which is a disadvantage when assessing a large animal population while trying to obtain consistent scoring of clinical signs.

Assessing and controlling diseases in swine production facilities is key for overall animal health and welfare, and to have a better-quality product at market. Disease control in swine continues to gain the attention in veterinary research due to financial losses and a general concern for food safety. Recently, researchers have aimed to understand host and virus miRNAs roles by sequencing and expression patterns. MiRNAs are small, ncRNAs approximately 22 nt in size, that regulate gene expression by targeting mRNAs for degradation or translational repression (Hammond, 2015).

E.coli-derived lipopolysaccharide (LPS) have been commonly used to induce systemic inflammatory response in numerous animal species (Nemzek et al., 2008). Lipopolysaccharide from a Gram-negative bacteria such as *E. coli* is a strong innate immune-activating stimulus which triggers a systemic inflammatory response and mimics key aspects of Gram-negative sepsis (Van Amersfoort, Van Berkel, & Kuiper,

2003). The LPS model previously has been used to identify candidate genes and potential biomarkers associated with systemic inflammation in human (Jayashree et al., 2014) and veterinary medicine (Peters et al., 2012).

Clinical observations outweigh biological analysis in the absence of a clear link between the laboratory findings and the clinical observation (Myers, Smith, & Turfle, 2017; Noh et al., 2009). The lack of a validated swine animal model prevents an accurate measurement for inflammation and inhibits the future development of effective drugs for swine (Peters et al., 2011). Identification of a reliable biomarker from a systemic inflammatory response needs to be easily obtained, safe, and provide the lowest risk of discomfort to the subject (Marshall & Reinhart, 2009). Proteins, metabolites, and RNA are the most common types of biomarkers used for drug development and disease predictors and detectors (Myers et al., 2017). Traditionally, urine and blood samples (plasma or serum) are the most commonly used tissues to assess changes in these analytes.

Recent studies suggest miRNAs are highly stable in extracellular fluids such as serum, plasma, and urine, and able to regulate gene expression without been rapidly degraded (Kroh et al., 2010; Weber et al., 2010). The measurement of the circulating cell-free form of miRNA is challenging due to a number of technical problems such as processing and extraction of RNA. Nonetheless, circulating miRNA concentrations may serve as biomarkers using plasma and serum miRNAs for prediction, or diagnosis, or determination of the severity of inflammation in swine. With real-time PCR methods researchers documented miRNA regulation in

Dachshunds dogs, and proposed its use as a diagnostic method for detecting endocardiosis, the most common heart disease in the breed. This technology helped identify different stages of the disease based on the reduced expression levels of certain biomarker miRNA (Hulanicka, Garncarz, Parzeniecka-Jaworska, & Jank, 2014). Here, our goal is to determine the best tool for inflammation analysis in swine.

Materials and Methods

Pigs

Fifty-nine (59) Yorkshire swine barrows weighing approximately 70 kg were used in the *in vivo E. coli* O55:B5 lipopolysaccharide (Sigma–Aldrich, St. Louis, MO) challenge. The experimental protocol was approved by the Animal Care and Use Committee at the Office of Research, Center for Veterinary Medicine, U.S. Food and Drug Administration, and all procedures were conducted in accordance with the principles stated in the Guide for the Care and Use of Laboratory Animals (2010) and the Animal Welfare Act of 1966 (P.L. 89-544), as amended.

Escherichia coli challenge and blood collection

The animals were randomly divided into six groups: No LPS challenged (n=12), LPS challenged 0.125 µg/kg body weight (n=13), LPS challenged 0.25 µg/kg body weight (n=14), LPS challenged 0.5 µg/kg body weight (n=6), LPS challenged 1.0 µg/kg body weight (n=6), and LPS challenged 2.0 µg/kg body weight (n=8). All swine received an indwelling vascular catheter for blood collection which eliminates the use of

mechanical restraints during the sampling process. LPS challenged groups were administered LPS (in sterile, pyrogen-free saline) derived from E. coli O55:B5 lipopolysaccharide (Sigma-Aldrich, St. Louis, MO) via the indwelling catheter. Blood samples were collected immediately prior to the challenge at 0 hr (baseline), and at 1, 3, 6, 8, and 24 hrs post LPS challenge. 30 ml of blood was collected and centrifuged immediately. For the preparation of plasma, whole blood samples were centrifuged at 4,000 x *g* at 4 °C for 15 minutes and the plasma removed. The plasma was then aliquoted into sterile 1.5 ml microcentrifuge tubes and stored at -80 °C until plasma microRNA analysis.

RNA isolation and reverse transcription

Total RNAs were extracted from plasma samples using the miRNeasy mini kit (Qiagen, Valencia, CA, USA). The procedure is a phenol/guanidine-based lysis and silica-membrane-based purification of the total RNA from the plasma samples. A miRNA mimic *C. elegans* miR-39 was added as a spiked-in control to determine the purification efficiency. The purification of the extracted total RNA was performed according to the manufacturer's instructions using the miRNeasy (Qiagen, Valencia, CA, USA) mini kit. The total RNAs were eluted in 14 µl RNase-free water. cDNA was generated using the miScript Reverse Transcription (RT) Kit (Qiagen, Valencia, CA, USA), according the manufacturer's instructions. 1.5 µl total RNA, 2 µl miScript Reverse Transcriptase Mix, and 4 µl miScript HiSpec RT buffer (Qiagen, Valencia, CA, USA) were mixed (Illustration 2). The mixture was incubated for 60 minutes at 37 °C, then for 5 minutes

at 95 °C to inactivate miScript Reverse Transcriptase Mix. 200 µl of RNase-free water was added to the reverse transcription product for dilution prior to PCR.

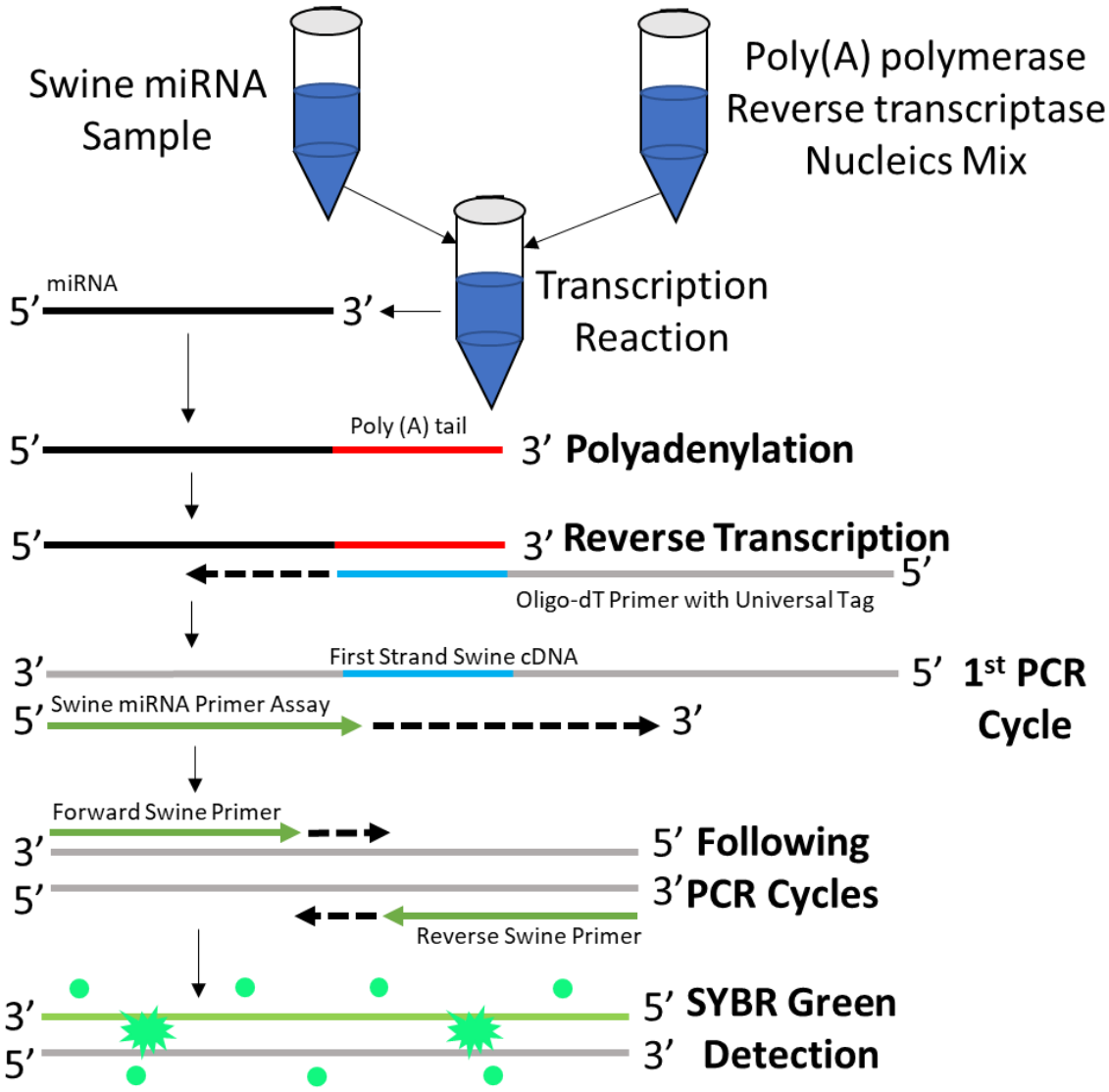

Illustration 2. General miScript miRNA PCR array workflow.
The poly(A) polymerase first polyadenylates the mature swine miRNAs in the sample. Each miRNA with a poly(A) is reverse transcribed to a cDNA using an oligo-DT primer. The forward and reverse swine primers of interest are quantified using a combination of SYBR green based detection and real-time PCR.

Quantitative RT-PCR

Quantitative real-time RT-PCR (qRT-PCR) was performed using miScript SYBR Green PCR Kit and miScript Primer Assays (Qiagen, Valencia, CA, USA) and PCR array workflow (Illustration 2). For the Pig miFinder miScript miRNA PCR Array (Qiagen, Valencia, CA, USA) analysis, aliquots of the reverse transcription product were placed in each well of the 96-well plate which contained the 84 abundant swine miRNAs. For further evaluation, specific primers for ssc-let-7e-5p, ssc-mir-22-3p, and ssc-miR-146a-5p from Qiagen (Qiagen, Valencia, CA, USA) were mixed with aliquots of the reverse transcription product in 96-well plates. Real-time detection was performed using Eppendorf's RealPlex4 (Eppendorf, Hauppauge, NY, USA) with the following PCR protocol: initial activation of HotStarTaq DNA Polymerase (95 °C, 15 min); 40 cycles of denaturation (94 °C, 15 sec), annealing (55 °C, 30 sec), and extension (70°C, 30 sec). The relative amount of each *C. elegans* miR-39 in PCR array analysis was normalized to an average of the *C. elegans* miR-39. Cycle threshold (Ct) values were recorded and data analysis was performed using software provided by the manufacturer.

Statistical analysis

Fold Changes were assessed using the comparative ΔΔCT method with normalization to a *C. elegans* miR-39 exogenous control (Livak & Schmittgen, 2001). Data are presented in comparison to the no LPS challenged control data, and as mean ± Standard error of the mean (SEM). Significant differences between two selected groups were

estimated using the unpaired student *t* test. A p-value ≤ 0.05 was considered statistically significant.

Results

Evaluation of microRNA profiles of swine plasma

An initial examination of changes in expression of plasma miRNAs was performed by Pig miFinder miRNA PCR array analysis between the swine control (n=6) and 2.0 µg/kg LPS treatment (n=5) group. *C. elegans* miR-39 miScript was added in the miRNA purification as a miScript PCR control and used for data normalization with the ΔΔCT method. A total of 41 miRNAs, 7 upregulated and 34 down-regulated, were identified with significant differential expression in the 2.0 µg/kg LPS treatment groups in comparison to the control group. The comparison of the non-LPS treated control and 2.0 µg/kg LPS raw array data was normalized, and a total of six miRNA were selected based on the highest degree of expression of either up or down-regulated values. This includes 3 (>3 folds; ssc-let-7e, ssc-let-7f and ssc-let-7a) that were significantly upregulated and 3 (>3 folds; ssc-miR-22-3p, ssc-miR-146a-5p, and ssc-miR-27b-3p) that were downregulated (Figure 5).

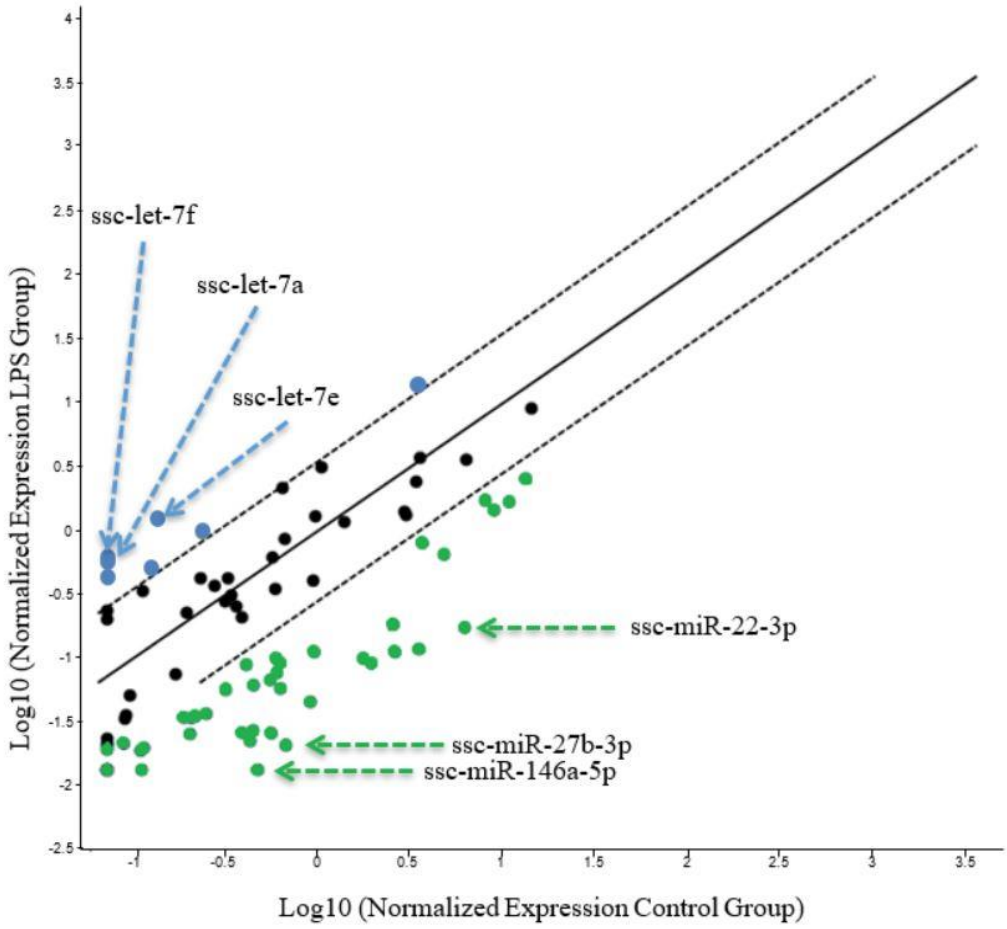

Figure 5. Control vs 2.0 µg/kg LPS PCR Array at 3 Hour. Scatter plot comparing the gene expression levels between the control and the 2.0 µg/kg LPS group at the 3 hr time point. The data points outside the dashed lines indicate fold-differences larger than the 3.5-fold threshold defined. The blue upper-left corner identified the up-regulated genes and the green symbols are the down-regulated genes

Although a miRNA pathway analysis database was not available for swine, predicted or experimentally verified common pathways and targets for human miRNAs were assessed using DIANA mirPATH v3.0 tool (Vlachos et al., 2012). In this heat map visualization, the darker colors represent the lower p-values, or higher significance, and is based on the common interaction compared to the overall pathway analysis in

order to provide insights into the similarities between human and swine miRNAs functionality (Figure 6).

To further investigate the results, these six differentially expressed miRNAs were analyzed by Quantitative Real Time RT-PCR (qRT-PCR) using the same miRNA samples (Table 5). In the initial single-run findings ssc-miR-22-3p and ssc-miR-27b-3p in the 2.0 µg/kg LPS treatment group were significantly downregulated at the 3 hr time point (Figure 5). However, after processing triplicates for the 2.0 µg/kg LPS treatment group; both ssc-miR-22-3p and ssc-miR-27b-3p unexpectedly exhibited an increase in gene expression at 3 hr and the largest change for 1 hr time points within experimental error (Figure 7A-B). Additionally, the ssc-miR-146a-5p levels in 2.0 µg/kg LPS group, increased between 0 and 3 hrs post-LPS. However, expression was downregulated with a decrease from 3 to 8 hrs (Figure 7C). Throughout the time course, the miRNA expressions for both ssc-let-7e (Figure 8A) and ssc-let-7f (Figure 8B) after 2.0 µg/kg LPS stimulation were greater than non-LPS control groups. The miRNAs ssc-let-7e and ssc-let-7f in the 2.0 µg/kg LPS group, recorded the largest margin of change at 3 hr from baseline Ct values (Figure 8A-B). The data gives insight into the time frame of the expression patterns of different plasma miRNAs during the 2.0 µg/kg LPS response as well as which elevated miRNAs would be best for diagnostic indication. However, the 2.0 µg/kg LPS dosage level produced an endotoxemic response that may or may not be indicative of an inflammatory response. Therefore, LPS dosage levels had to be reassessed. An LPS dose-ranging study was initiated.

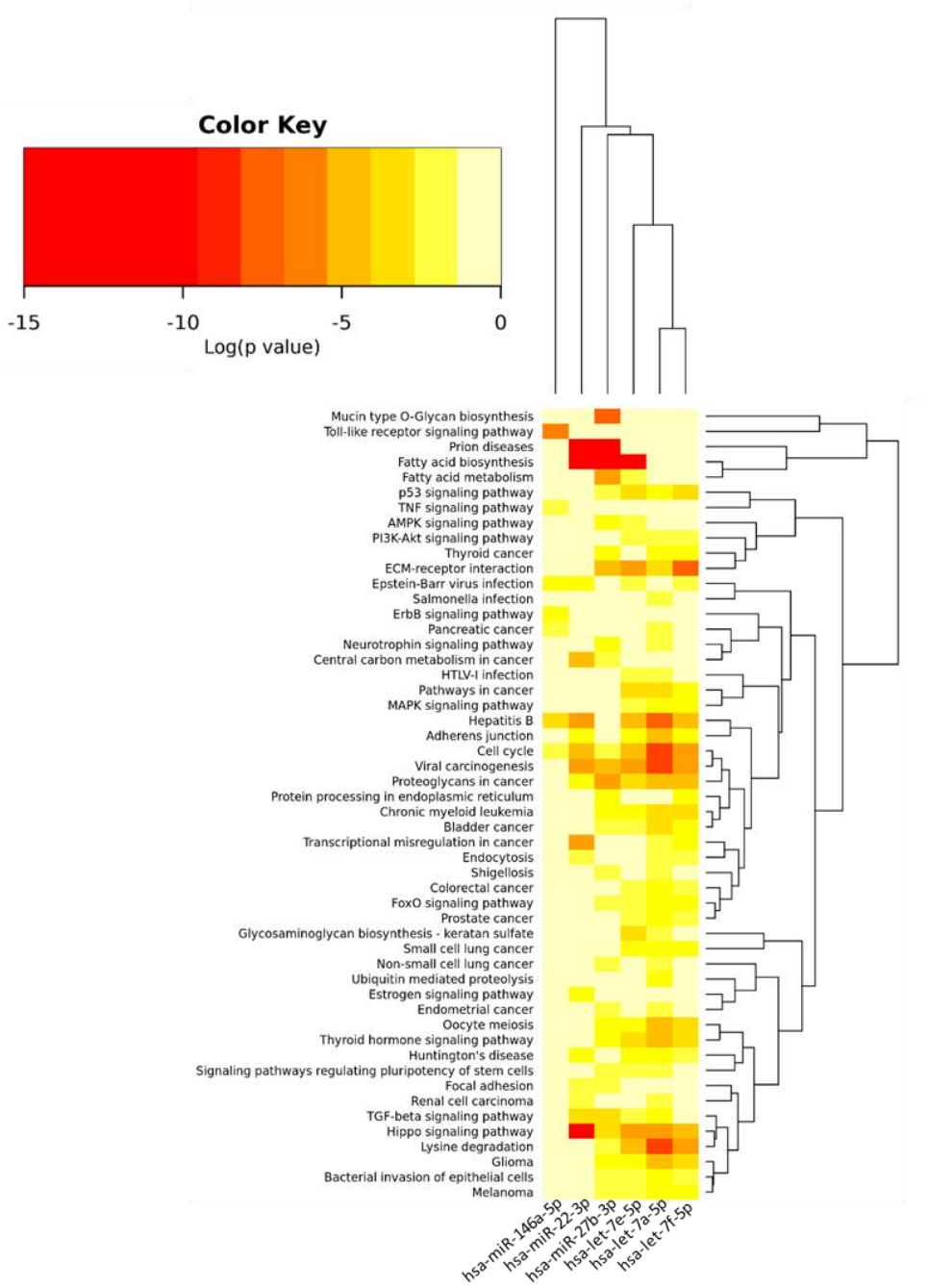

Figure 6. Heat map of miRNAs and pathways The cluster analysis while using the absolute *P*-values in its calculation the DIANA-miRPath v2.0 server created visualization of the known human miRNAs and pathways. The red on the spectrum represents the lower significant values and very small *P*-values. This tool was used to explore common miRNA-pathway relationship or similar targets with each potential biomarker miRNAs of interest.

Table 5. miRNA Family Functions

Selected miRNA differentially expressed in plasma samples from post 2.0 µg/kg LPS treatment group

Accession No.	miRNA	Biological Family Function	PMID
Up-regulated			
MI0013086	ssc-let-7e	Involved in oncogene expression	[19917043] [20180025]
MIMAT0002152	ssc-let-7f	Involved in mammalian embryonic development	[15885146]
MIMAT0013865	ssc-let-7a	Involved in oncogene expression	[19917043] [20180025]
Down-regulated			
MIMAT0015710	ssc-miR-22-3p	Post-transcriptionally regulate gene expression	[19917043] [20180025]
MIMAT0022963	ssc-miR-146a-5p	Involved in the regulation of inflammation; function in the innate immune system	[20433717] [21312241]
MIMAT0013890	ssc-miR-27b-3p	Operates together with miR-23 and mir-24 in a co-operative cluster	[19917043] [20180025]

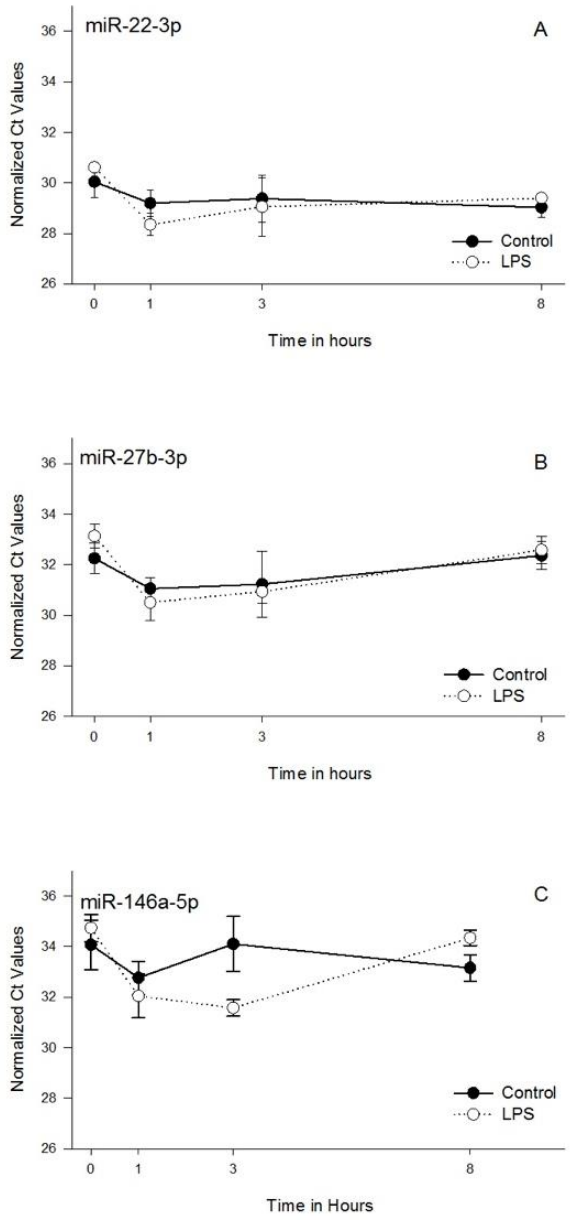

Figure 7. Expression levels of miRNAs at 2.0 µg/kg LPS. Control and 2.0 µg/kg LPS plots at 0 hr, 1 hr, 3 hr, and 8 hr for the mean gene expression levels of miRNAs miR-22-3p (A), miR-27b-3p (B), and miR-146a-5p (C). Error bars represent the standard error of the mean (SEM).

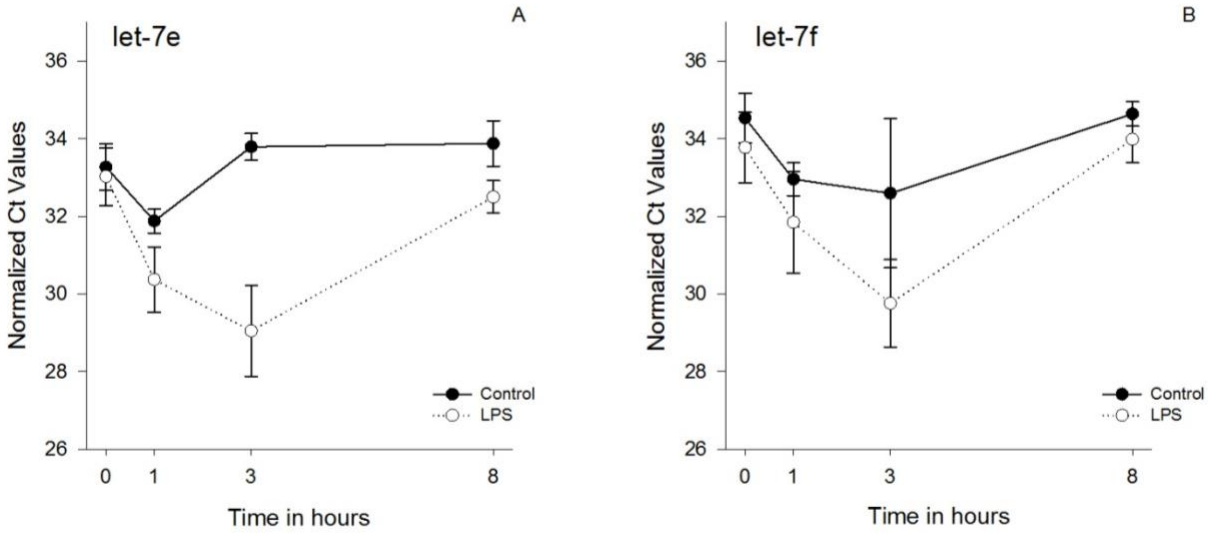

Figure 8. Expression levels of miRNAs at 2.0 µg/kg LPS. Control and 2.0 µg/kg LPS plots at 0 hr, 1 hr, 3 hr, and 8 hr for the mean gene expression levels of miRNAs let-7e (A) and let-7f (B). Error bars represent the standard error of the mean (SEM).

Changes in miRNA expression levels between control and LPS dosages

The correlation of fold changes in expression in the control and the LPS dosages levels was used to determine the consistency, accuracy, and reliability of the evaluation. Clinical signs and the severe morbidity of the swine confirmed the 2.0 µg/kg treatment group to be endotoxemic. Further expression analysis of let-7e, let-7f, miR-22-3p, miR-146a-5p, and ssc-miR-27b-3p were examined following each LPS dosage stimulation. Ideally, in this current study, the differential expression of a potential miRNA inflammation biomarker would correlate with the different LPS dosage levels. Although significant differences were seen in the 2.0 µg/kg LPS stimulation for let-7f, miR-146a-5p, and ssc-miR-27b-3p expression compared to

control, there was no detectable correlation between miRNA changes and LPS dosage groups (data not shown).

Only the miRNA profiles of ssc-let-7e-5p and ssc-miR-22-3p for each LPS dosage were found to have differentially expressed trends in comparison to the non-LPS control groups (Figure 9 and 10). The miRNA expression for ssc-let-7e-5p and ssc-miR-22-3p were both shown to be significantly ($p<0.05$) upregulated for all times for the 2.0 µg/kg treatment group (Figure 9 and 10). Other than the 2.0 µg/kg treatment, 0.125 µg/kg at 0 and 8 hr were the only upregulated expression for ssc-let-7e-5p (Figure 9). Additionally, upregulation outside of the 2.0 µg/kg treatment group for ssc-miR-22-3p was only seen for the 1.0 µg/kg treatment group at 8 hr (Figure 10). At 1 hr post-LPS, ssc-let-7e-5p decreased as the LPS dosage levels increased from 0.125 to 1.0 µg/kg compared to the control treatment group (Figure 8). Similarly, as the LPS doses increased from 0.125 to 0.5 µg/kg, ssc-miR-22-3p levels significantly decreased at 1 hr post-LPS (Figure 10). Therefore, the miRNA expression levels of LPS dosages from 0.125 µg/kg to 1.0 µg/kg from this study could be used to distinguish the severity of inflammation. Additionally, the miRNA profiles observed for the 2.0 µg/kg LPS dosage stimulation may be potential biomarkers for endotoxemia.

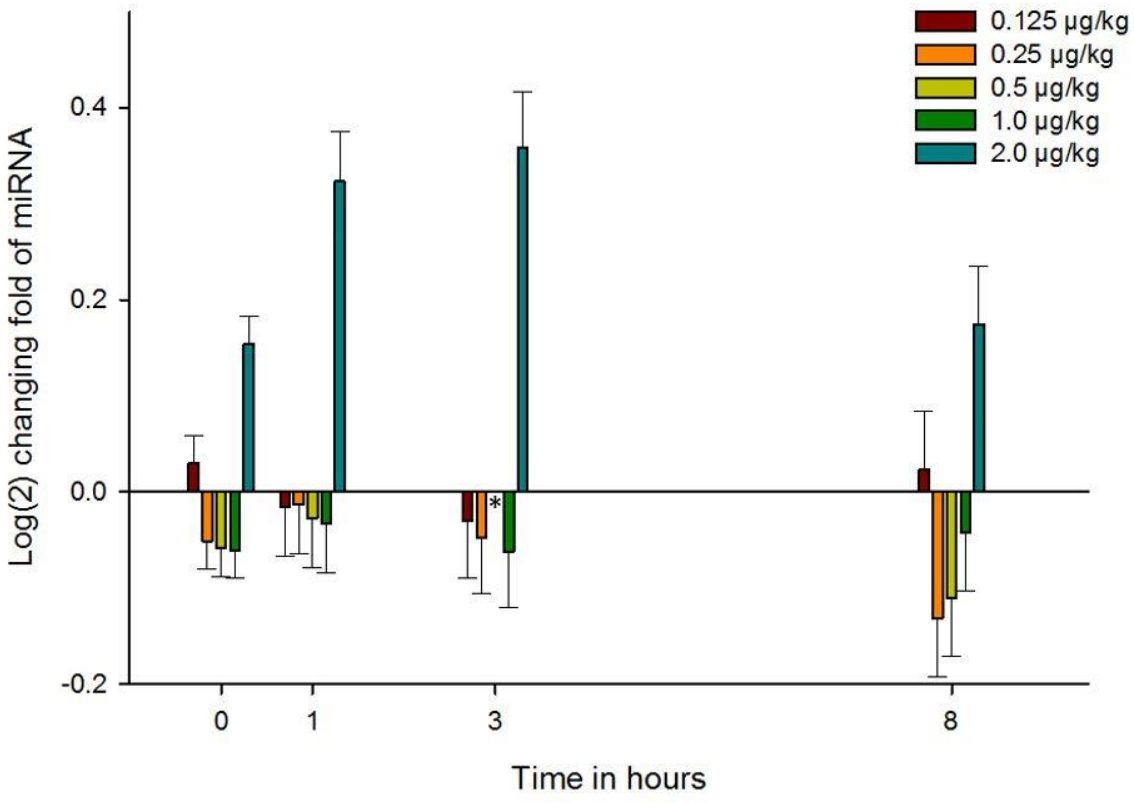

Figure 9. Let-7e fold change expression levels of control vs LPS dosages. Control vs 0.125, 0.25, 0.5, 1.0, and 2.0 µg/kg LPS treatment groups plot at 0, 1, 3, and 8 hr for the mean gene expression levels of miRNAs Let-7e. Error bars represent the standard error of the mean (SEM). *The let-7e relative expression values for 0.5 ug were non-detectable at 3 hr.

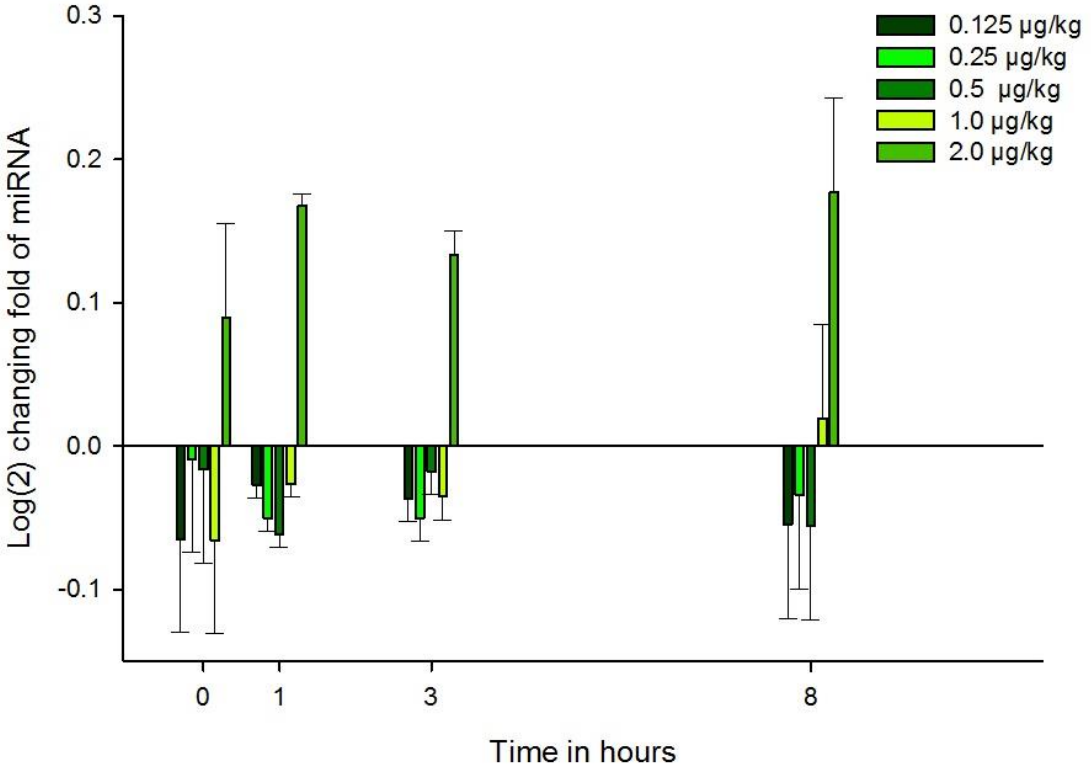

Figure 10. miR-22-3p fold change expression levels of control vs LPS dosages
Control vs 0.125, 0.25, 0.5, 1.0, and 2.0 µg/kg LPS treatment groups plot at 0, 1, 3, and 8 hr for the mean gene expression levels of miRNAs miR-22-3p. Error bars represent the standard error of the mean (SEM).

Discussion

MicroRNA expression strategies were used to assess the response to the experimental administration of LPS in swine. There are several infection models that have been developed to reproduce aspects of inflammation based on the administration of a toxin, pathogen, or changes to the animal's endogenous protective barrier (Stortz et al., 2017). The toxemia animal models have been commonly used to mimic clinical aspects of the sepsis process (Doi, Leelahavanichkul, Yuen, & Star, 2009). The aim of the study was to explore the use of miRNAs as biomarkers for

monitoring significant differential expressions that result from inflammation and endotoxemia. The use of circulating miRNAs as a non-invasive biomarker has potential, in comparison to other RNA molecules that are unstable in plasma (Rice et al., 2015). MiRNAs can be resistant to RNase activity and remain stable in extreme pH which is ideal for a practical biomarker (Gilad et al., 2008). In order to properly investigate and assess the miRNA levels accurately, it was important to take into consideration the handling and processing of the samples. A previous study documents how to obtain consistent results, reduce variability, and increase reproducibility in miRNA expression data. Strategies suggested include EDTA collection tubes and separating plasma fractions from whole blood samples before -80°C storage (Glinge et al., 2017). In this work we followed those guidelines because repeatability and reliability in downstream analysis of the miRNA expression results were essential for determining if miRNAs could be used as a biological indicator in swine.

The current study examined the temporal expression patterns of selected miRNAs in plasma samples from non-LPS treated control swine, compared with those swine dosed at incremental LPS levels. Using an *in vivo* swine model system, we demonstrated the involvement of several microRNAs (let-7e-5p, miR-22-3p, miR-146a and others) in systemic inflammatory responses.

The let-7 family in mouse models as well as miR-22 human studies have known roles in the regulation of inflammatory responses (Brennan et al., 2017; B. Chen et al., 2016). Results from our endotoxemia studies showed that LPS treatment

group demonstrated upregulation of let-7e and let-7f during the peak of stimulation. In endothelial cells, let-7e increased NF-kβ activity by targeting genes in the NF-kβ pathway and played a pro-inflammatory role in an earlier study (Lin et al., 2017). The overexpression of miR-22 has been shown to increase the synthesis of several cytokines such as IL-1β, IL-6, and IL-8 in the endothelial cell type as well (Gu et al., 2017). Another study has shown upregulation of let-7e-5p, which targets TLR4, by protein kinase AKT1 in lipopolysaccharides-activated macrophages (Androulidaki et al., 2009).

Although our dose-ranging study expression data were conflicting, this effect could be due to roles in specific responses and various targets in different cell types (Ardekani & Naeini, 2010). Mammalian studies have shown that most let-7 miRNA family members are post-transcriptionally regulated by Lin28 and during inflammation, let-7 levels were reduced by NF-kβ upregulating of Lin28 (Kumar et al., 2011; Newman, Thomson, & Hammond, 2008). The downregulation of miR-22 expression occurred when inflammatory cells were stimulated with Polyinosinic:polycytidylic acid (Poly I:C) which suggests its role in the host inflammatory response (Gidlof et al., 2015). The severity of inflammation by LPS disease in swine is assessed and measured by the miRNA expression levels of both ssc-let-7e-5p and ssc-miR-22-3p.

Additionally, interest in miR-146 has increased in recent years due to its involvement with validated target genes of inflammation. Studies have shown that LPS stimulation in cell lines, which is recognized by TLR4, increases miR-146a

expression because it has a NF-kβ dependent gene within this pathway (K. D. Taganov, M. P. Boldin, K. J. Chang, & D. Baltimore, 2006). In immune cells following TLR activation by bacterial pathogens, miR-146a will then act as an anti-inflammatory miRNA by inhibiting TNFR-associated factor 6 (TRAF6) and IL-1R-associated kinase 1 (IRAK1) within a negative feedback loop (Alexander & O'Connell, 2015). Therefore, miR-146a plays the role of additional inflammation prevention in this TLR signaling pathway. Interestingly, the downregulation of circulating miR-146a has been mentioned as an indication of sepsis in plasma (L. Wang et al., 2013), yet in another study it is unable to exhibit differential expression of miR-146a in sepsis plasma samples (Puskarich et al., 2015). miR-146a could be associated with many pathologies that are involved in inflammatory responses. Our results demonstrated the upregulation of ssc-miR-146a-5p expression may be used as an indicator to determine endotoxemia in swine.

Chapter 6: Effects of swine microRNA mimics with Lipopolysaccharide (LPS) induced endotoxemia changes in 3D4/21 cells

Abstract

There have been limited studies focused on validation of swine miRNA with mRNA targets. The objective of this study was to validate a defined set of targets using artificial miRNA mimics transfected into cell lines to confirm specific targets of endogenous miRNAs after administration of *E.coli* lipopolysaccharide. Sixteen hours after mimic transfection of 3D4/21 cell lines, the cells were stimulated with 1 μg/ml LPS or phosphate-buffered saline (PBS). The cells were harvested and collected at 0, 1, 3, and 8 hrs post-administration. The selected genes DAD1, IL8, and ESR, which are involved in known pathways of inflammation, are predicted or validated human targets of either miR-146a, let-7a, or miR-22-3p. These were then evaluated by qRT-PCR to verify microRNA-mRNA interaction in swine. Using the ROX reference dye, mRNA changes in expression were assessed using the comparative ΔΔCT method for normalization against the PBS control group. DAD1 and ESR1 were negatively regulated by miR-22-3p and miR-146a-5p, respectively in 3D4/21 cells after LPS stimulation. However, miR-146a-5p may play an indirect positive regulatory role in both DAD1 and IL8 mRNA expression. Furthermore, we found an inverse relationship between LPS stimulation compared with the let-7a-5p overexpression

with DAD1. Our endotoxemia study provides new evidence on the roles and predicted targets of miR-146a, let-7a, and miR-22-3p in swine.

Introduction

The inflammatory response is a complex cascade of processes initiated by diverse triggers such as bacteria, toxins, and injury. Inflammation is the biological response to tissue injury or pathogens and is involved in the host's defensive mechanism. Severe morbidity and mortality are associated with endotoxemia, which has inflammation as an early sign. Sepsis has been defined as life-threatening organ dysfunction by systemic inflammatory responses syndrome resulting from infection (Gül et al., 2017). The key difference between sepsis and endotoxemia is the latter is caused by a single component such as LPS, while the former is due to multiple bacterial components.

Previous work from this laboratory identified several swine mRNAs whose expression was altered following *in vivo* exposure to LPS (Peters et al., 2012). As they belonged to diverse cellular pathways, changes in miRNA were subsequently examined to determine if there was a common regulatory mechanism underlying the inflammatory induced changes in mRNA expression. Those results identified three miRNAs associated with inflammatory processes that were altered as a consequence of *in vivo* LPS exposure (Swain, Deaver, Lewandowski, & Myers, Manuscript submitted for publication). Those results further suggest that ssc-let-7a-5p, ssc-miR-

22-3p and ssc-miR-146a-5p swine miRNAs could be potential biomarkers for LPS-stimulation to induce inflammation in swine.

Current knowledge of the mRNA targets for miRNA control is based on information derived from human mRNA/miRNA research. Synthesized miRNA mimics are used to study mechanisms of miRNAs by cell transfection and are designed to mimic the function of endogenous miRNAs (Huang, Zhu, & Li, 2015). Information on whether those results can reliably predict swine miRNA control is lacking. Accordingly, this study was initiated to begin addressing that gap. The low level of endogenous miRNA in a porcine alveolar macrophage cell line (3D4/21), coupled with the high target gene expression, established mimic miRNAs as a suitable approach for confirming mRNA targets. This study is an evaluation of the roles of ssc-let-7a-5p, ssc-miR-22-3p, and ssc-miR-146a-5p miRNAs in inflammation induced by LPS in swine.

In addition, the experimental results confirmed that selected swine miRNA-mRNA targets were as predicted based on the human miRNA-mRNA target database. Since miRNAs are known to be highly specific in certain cells or tissues, even the same disease or response may have a different miRNA expression pattern or mRNA target. Our results together with the current database information about the selected miRNAs and mRNA compare functionality as a result of inflammation.

Materials and Methods

Cell Culture

The swine macrophage lung cell line 3D4/21 ATCC® CRL-2843TM (American Type Culture Collection, Manassas, VA, USA) was cultured in the complete growth medium of RPMI-1640 (Thermo Fisher Scientific; Waltham, MA, USA) medium supplemented with 10% fetal bovine serum (Thermo Fisher Scientific; Waltham, MA, USA). The cells were grown at 37 °C in 5% CO_2. The media was replaced and replenished until growth of 80-100% confluency was reached, then culture medium would be discarded. 2.0 ml solution of 0.25% (w/v) Trypsin and 0.53 nM EDTA (Thermo Fisher Scientific; Waltham, MA, USA) was added to the cell layer of the T-75 flask for resuspension. 16.5 ml of complete media was added to the resuspended cell flask. 5 ml of the resuspended cells were added to four separate T-75 cell culture flasks containing 15 ml of complete growth medium for sub-culturing. The media would be replaced and replenished again until growth of 80-100% confluency was reached, then the culture medium would be discarded. 2.0 ml of 0.25% (w/v) Trypsin and 0.53 nM EDTA and 15 ml of complete growth was added to each flask and then combined into one T-75 cell culture flask. 20 µl from the combined cell culture was added to 180 µl of trypan blue (Thermo Fisher Scientific; Waltham, MA, USA) in a tube. 20 µl of the solution was then added to a cellometer disposable counting chamber and counted under a microscope. After a density of $1.0x10^5$ cells per well

was adjusted with complete growth medium, 500 µl of the total cell culture was plated in 24 well-plates.

Cell transfection with Swine miRNA mimic, Human miR-1 positive control mimic, and AllStars Negative control siRNA

Cell transfection procedure was performed using HiPerFect Transfection (Qiagen, Valencia, CA, USA) according to the manufacturer's instructions. Reconstituted MiScript miRNA mimics of ssc-miR-146a, ssc-let-7a, ssc-miR-22-3p, hsa-miR-1-3p positive control and AllStars negative control siRNA (Qiagen, Valencia, CA, USA) were dissolved in RNase free water to make a 20 µM stock for each. The synthetic miRNA hsa-miR-1 mimic was used as a positive control since hsa-miR-1 is expressed in muscle and rarely in other cell types. Separate complexes of 0.15 µl of the mimic or control with 3 µl of HiPerFect were diluted in 100 µl Eagle's Minimum Essential Medium ATCC® 30-2003™ (American Type Culture Collection, Manassas, VA, USA) culture without Fetal bovine serum. The culture medium samples were incubated for 5-10 min at room temperature prior to transfection. The complex was then added dropwise to the appropriate sample culture well and the final concentration for the mimic or control was 5 nM. Cell wells that did not contain a mimic or control small interfering RNA (siRNA) received only a complex with HiPerFect and serum free culture. Each 24-well plate was then swirled to ensure uniform distribution of the transfection complexes and placed in the incubator at 37 °C in an atmosphere of 5% CO_2 for 16 hrs.

Cell Treatment and RNA isolation After the initial 16 hr incubation, the 0 hr baseline plate was removed and the cells were collected prior to the lipopolysaccharide (LPS) *Escherichia coli* O55:B5 (Sigma-Aldrich, MO, USA) or phosphate-buffered saline (HyClone, UT, USA) administration. The cell culture plates were then stimulated with 1 μg/ml LPS or phosphate-buffered saline (PBS) and incubated until collection at either the 1, 3, or 8 hr time point. Total RNAs were extracted using the RNeasy Plus mini kit (Qiagen, Valencia, CA, USA) from the cultured cells according to the manufacturer's protocol. The cells were harvested by aspirating the medium and washed with PBS. The PBS was then aspirated and 200 μl of 0.25% trypsin in PBS was added to detach the cell from the plate. After detachment, 400 μl of complete media with serum was added and the cells were transferred to a 2 ml polypropylene centrifuge tube. The sample was then centrifuged at 300 x *g* for 5 min and the supernatant was aspirated completely. Cell pellets were either stored at -70 °C for later use or disrupted immediately. If the cell pellet was frozen, it was incubated in a water bath at 37 °C until it was completely thawed. 2.2 ml of β-mercaptoethanol (β-ME) was added to 220 ml of Buffer RLT Plus for a working solution. Based on the number of pelleted cells, 350 ml of Buffer RLT Plus was added to each pellet to disrupt the cells. After vortex, the samples were then transferred directly into a QIAshredder (Qiagen, Valencia, CA, USA) spin column placed in a 2 ml collection tube. The samples were centrifuged at 20,000 x *g* for 2 min at 25 °C and the homogenized lysate was transferred to a gDNA Eliminator (Qiagen, Valencia, CA,

USA) spin column in a 2 ml collection tube. The samples were centrifuged at 20,000 x *g* for 30 sec at 25 °C and repeated centrifugation until all liquid has passed through the membrane. The gDNA Eliminator spin column was discarded and the flow-through was saved. 350 µl of 70% ethanol was added to the flow-through and mixed well by pipetting. A maximum of 700 µl of each sample was transferred to a RNeasy (Qiagen, Valencia, CA, USA) spin column in a 2 ml collection tube. The samples were centrifuged at 20,000 x *g* for 20 sec and the flow-through was discarded. 700 µl wash Buffer RW1 (Qiagen, Valencia, CA, USA) was added to the RNeasy spin column and centrifuged at 20,000 x *g* for 20 s. The flow-through was discarded and 500 µl wash Buffer RPE (Qiagen, Valencia, CA, USA) was added to the RNeasy spin column. The samples were centrifuged at 20,000 x *g* for 2 min to wash the spin column and then the flow-through was discarded. Another 500 µl wash Buffer RPE was added to the RNeasy spin column and was centrifuged at 20,000 x *g* for 2 min. The collection tube including the flow-through was discarded and the RNeasy spin column was placed in a new 2 ml collection tube. The sample was centrifuged at 20,000 x *g* for 1 min and the RNeasy spin column was placed in a new 1.5 ml collection tube. 50 µl of RNase-free water was added directly to the spin column and centrifuged at 20,000 x *g* for 1 min at 25 °C to elute the RNA. The purified RNA was stored at either -20 °C or -80 °C in the RNase-free water.

RNA concentration and reverse-transcription

The concentration of the RNA and the 260/280 OD ratio ($OD_{260/280}$) was determined by loading 1 µl of the sample on a spectrophotometer. The ratio was used to determine the purity of the RNA with respect to contaminants that can absorb UV light. The sample replicates with the highest RNA concentration within the acceptable ratio (~2.0) were selected and diluted to 3 ng/µL with RNase-free water. The cDNA synthesis and genomic DNA elimination for the RNA samples procedure was performed using RT^2 First Strand kit (Qiagen, Valencia, CA, USA). In each PCR tube 3 ng total RNA sample, 2 µL Buffer GE (Qiagen, Valencia, CA, USA), and the appropriate volume of RNase-free water was added to reach a total volume of 10 µL. The PCR tube was then incubated for 5 min at 42 °C and placed directly on ice for 1 min. The reverse-transcription reaction mix was prepared with 4 µL 5x Buffer BC3 (Qiagen, Valencia, CA, USA), 1 µL Control P2 (Qiagen, Valencia, CA, USA), 2 µL RE3 Reverse Transcriptase (Qiagen, Valencia, CA, USA) mix and 3 µL RNase-Free water according to the manufacturer's instructions. 10 µL of the reverse-transcription mix was added to each PCR tube containing the 10 µL of genomic DNA elimination mix. The solution was mixed gently by pipetting and incubating for 15 min at 4 2°C. 91 µL of RNase-free water was added to each reaction and mixed by pipetting up and down. The reactions were either stored at -20 °C or placed on ice prior to proceeding with real-time PCR.

Quantitative RT-PCR of DAD1, Il-8, ESR1, and HDAC4 expression

Quantitative real-time RT-PCR (qRT-PCR) was performed using miScript SYBR Green ROX^{TM} PCR Kit and RT^{2} qPCR Primer Assays (Qiagen, Valencia, CA, USA). For evaluation, specific primers for Pig Defender Against Cell Death 1 (DAD1), Pig Interleukin-8 (IL8), Human Estrogen Receptor 1 (ESR1), and Human Histone Deacetylase 4 (HDAC4) from Qiagen (Qiagen, Valencia, CA, USA) were mixed with aliquots of the reverse transcription product in 96-well plates. The quantitative Real-time PCR reaction contained 12.5 µl SYBR Green ROX^{TM} Master mix, 1 µl cDNA, 1 µl specific RT² qPCR primer, and 10.5 µl RNase-free water. Real-time detection was performed using Eppendorf's RealPlex4 (Eppendorf, Hauppauge, NY, USA) with the following PCR protocol: initial activation of HotStarTaq DNA Polymerase (95 °C, 10 min); 40 cycles of fluorescence data collection (95 °C, 15 sec then 60 °C, 1 min). The melting curve program was performed with the initial denaturation step (95 °C, 15 sec), a melting curve step from 60 to 95 °C (Ramp time 20 min), and then a final temperature step (95 °C, 15 sec) for each well. The relative amount of ROX reference dye in each PCR array analysis was used to normalize fluorescence across all the samples. Cycle threshold (Ct) values were recorded and data analysis was performed using software provided by the manufacturer.

Statistical analysis

Fold changes were assessed using the comparative CT Method (ΔΔCT method) for normalization with ROX reference dye (Livak & Schmittgen, 2001). Data are

presented as mean ± SEM. Data is presented in comparison to the no LPS challenged control data. Significant differences between two selected groups were evaluated using the unpaired student *t* test. A p-value ≤ 0.05 was considered statistically significant.

Results

Evaluation of mimic transfection in 3D4/21 cells

To ensure experimental system was working, the positive control miRNA mimic syn-hsa-miR-1-3p was transfected into 3D4/21 cells. The HDAC4 expression profiles with PBS or the positive mimic were generated at 0, 1, 3, and 8 hrs after treatment initiation in 3D4/21 cells (Figure 11). Cells treated with only PBS were used as a control. Syn-hsa-miR-1-3p miRNA mimic was used as a positive control in the cell culture study. The effect of hsa-miR-1 was analyzed by assessing the gene expression of its known target, HDAC4. The expected outcome would be reduced gene expression of HDAC4 after the transfection of the syn-hsa-miR-1-3p miRNA positive control mimic. The downregulated HDAC4 expression results after transfection of syn-hsa-miR-1-3p miRNA positive control mimic, compared to the control PBS without the positive control mimic, confirmed an effective miRNA transfection mimic protocol (Figure 11).

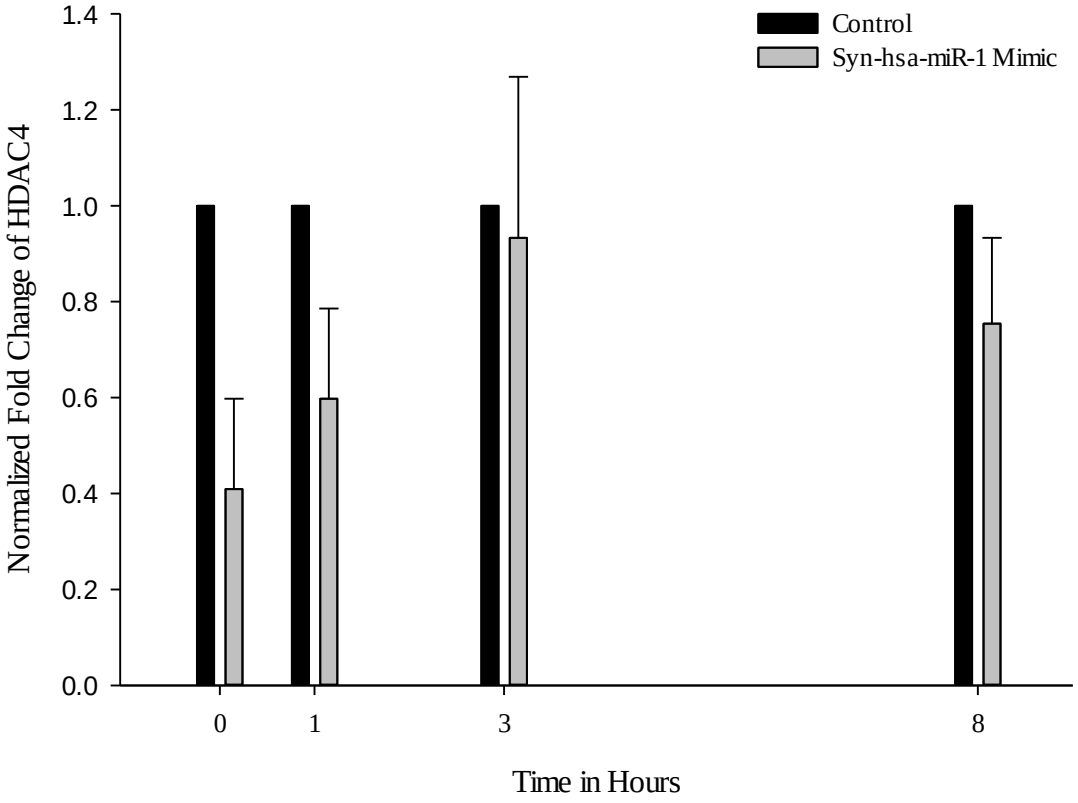

Figure 11. Selected primers for RT-PCR Detection for each treatment group. The 3D4/21 cells were analyzed for the specific temporal mRNA expression level changes after 1 µg/ml LPS or PBS stimulation.

Relative expression of DAD1, ESR1 and IL8 in 3D4/21 cells

The overall control and LPS induced expression patterns were assessed as a function of time, and the fold change for DAD1, ESR1 and IL8 genes were detected by qRT-PCR in the PBS stimulated 3D4/21 cells (Figure 12 and 13). These control temporal expression values were used to establish a baseline for the comparison to gene expression after LPS stimulation (Figure 12 and 13). The relative expression patterns for each selected mRNAs were calculated against the HDAC4 expression values

using the comparative Ct (ΔΔCt) value method. The temporal comparison of the HDAC4 values against each DAD1, ESR1 and IL8 gene in the PBS control group were used to assess the changes within the cell culture, independent of the LPS treatment (Figure 12). In the PBS control groups, IL8 expression appeared relatively stable throughout the time course. However, DAD1 and ESR1 were both significantly downregulated, with the greatest fold changes from 1 to 3 hr (Figure 12). DAD1 and ESR1 fold changes were upregulated from 0 to 1 hr compared to the slight downregulation for IL8 in the PBS control group. Changes in gene expression patterns after LPS administration were assessed in the cell line over the course of the stimulation (Figure 13). The relative expression pattern of ESR1 in the LPS stimulated group continuously decreased over time (Figure 13). Furthermore, DAD1 with LPS exhibited similar trends in comparison to the control group; however, for IL8 there was an apparent inverse correlation for expression (Figure 13). The expression patterns were used to assess the effect of each miRNA mimic on the cells after each treatment group.

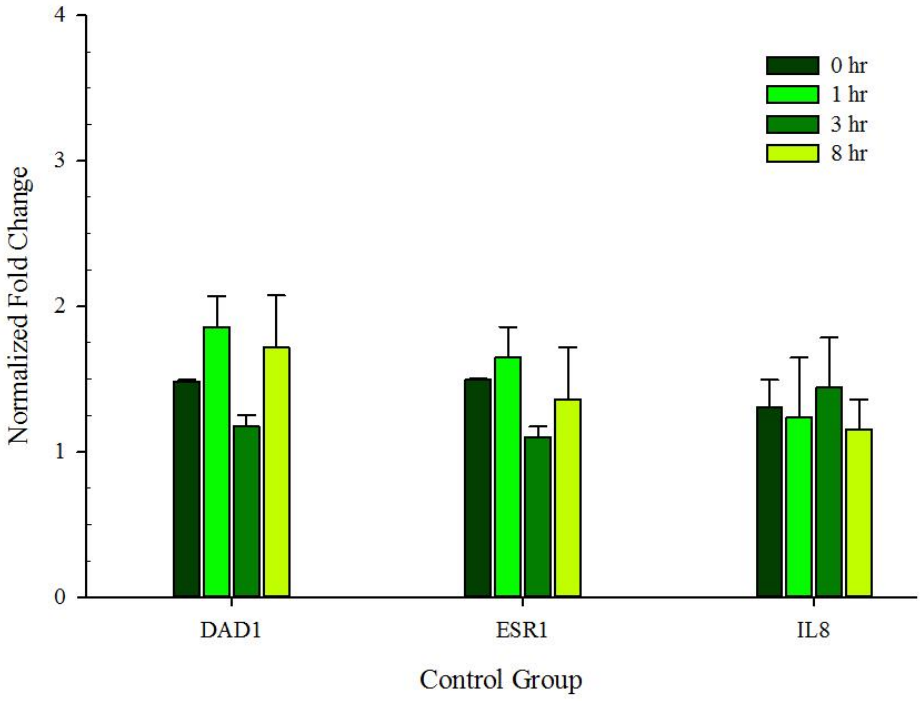

Figure 12. Control mean gene expression levels in 3D4/21. DAD1, ESR1, and IL8 mean gene expression levels at 0, 1, 3, and 8 hr in 3D4/21 in control group. Relative mean expression levels were calculated using a comparative Ct (ΔΔCt) value against HDAC4 values. Error bars represent the standard error of the mean (SEM).

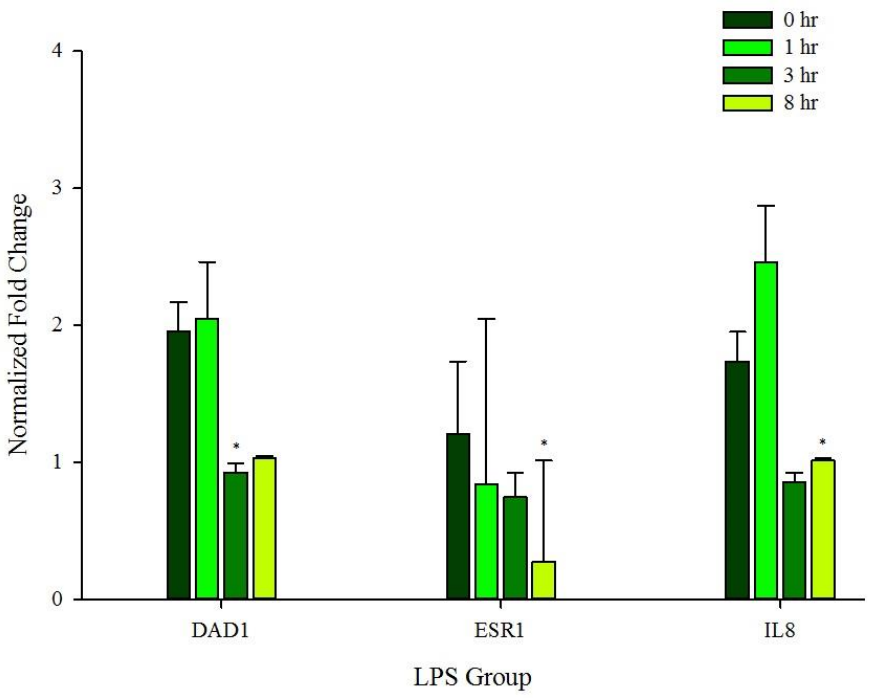

Figure 13. LPS treatment mean gene expression levels in 3D4/21. DAD1, ESR1, and IL8 mean gene expression levels at 0, 1, 3, and 8 hr in 3D4/21 in the LPS group. Relative mean expression levels were calculated using a comparative Ct (ΔΔCt) value against HDAC4 values. Error bars represent the standard error of the mean (SEM). *Indicates a significant difference to the comparison of control at each corresponding LPS time point (P>0.05).

Upregulation of DAD1 gene expression by miR-22-3p after LPS stimulation

To examine the effect of each miRNA in 3D4/21 cells, each mimic was separately transfected, and the predicted mRNA targets were analyzed by qRT-PCR (Figure 14-18). The cells containing each mimic were stimulated with LPS and then collected at 0, 1, 3, and 8 hrs after stimulation. After LPS stimulation, the DAD1 gene expression change was up-regulated. Additionally, LPS with the miR-22-3p mimic group followed a similar trend as the LPS only group, as both increased at 1 and 8 hrs, while

decreasing at 3 hr (Figure 14). Results indicated miR-22-3p mimic downregulated DAD1 after LPS stimulation. Although within experimental error, DAD1 expression of LPS with miR-22-3p mimic differ from normal levels of only LPS at the 8 hr timepoint (Figure 14).

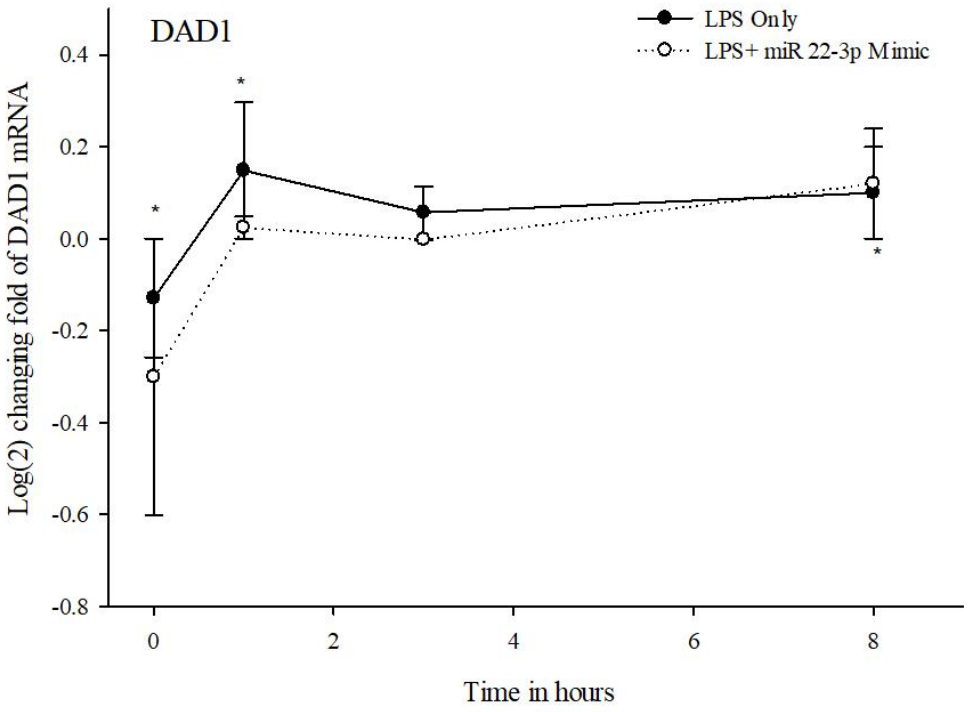

Figure 14. DAD1 gene expression with miR-22-3p mimic. DAD1 mean gene expression at 0, 1, 3, and 8 hr after 1 μg/ml LPS stimulation or LPS stimulation with miR-22-3p mimic. The mean gene expression data is normalized against the temporal fold changes of its control group. Error bars represent the standard error of the mean (SEM). *Statistical differences based on the comparison of control at each corresponding time point (P>0.05).

Downregulation of ESR1 gene expression by miR-146a-5p with LPS

In contrast to the trends showed with DAD1 and the miR-22-3p mimic, ESR1 gene expression were down-regulated for both LPS only group as well as with the miR-146a-5p mimic after LPS stimulation (Figure 15). LPS only and LPS with miR-146a-5p mimic groups both decreased at 1 and 8 hrs, while increasing slightly at 3 hr (Figure 15). However, the specific down-regulation of ESR1 from miR-22-3p mimic compared to the LPS only group from 0 to 3 hr is confirmation of gene regulation of ESR1. At the 8 hr time point, while LPS with miR-22-3p mimic appear to increase above the ESR1 expression levels of the LPS only group, it was within the experimental error (Figure 15).

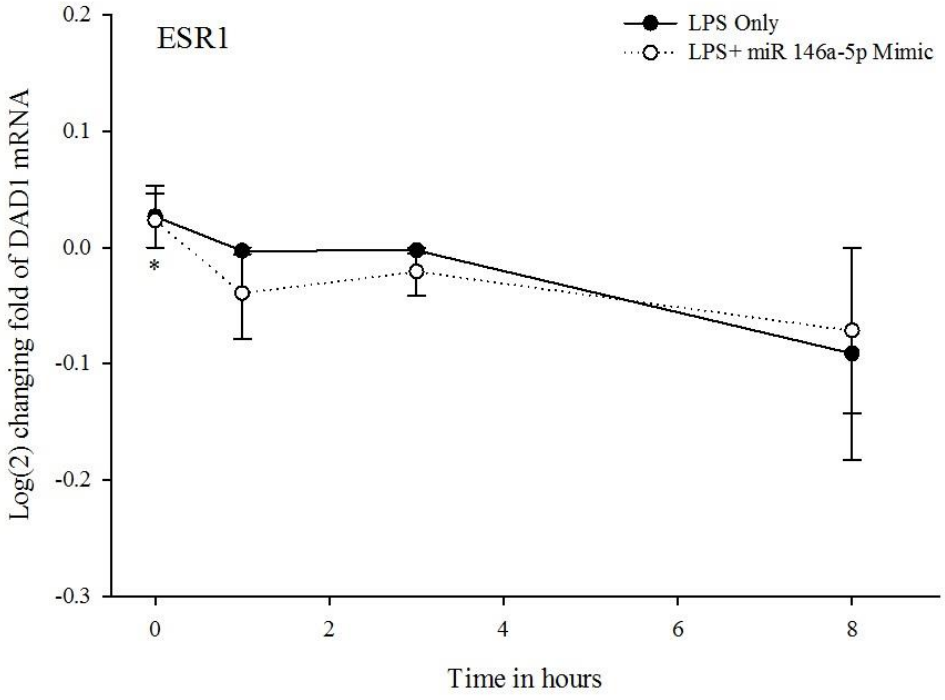

Figure 15. ESR1 gene expression with miR-146a-5p mimic. ESR1 mean gene expression at 0, 1, 3, and 8 hr after 1 μg/ml LPS stimulation or LPS stimulation with miR-146a-5p mimic. The mean gene expression data is normalized against the temporal fold changes of its control group. Error bars represent the standard error of the mean (SEM). *Statistical differences based on the comparison of control at each corresponding time point (P>0.05).

Regulatory role of miR-146a-5p with DAD1 and IL8 after LPS Stimulation.

Accordingly, after LPS stimulation, the miR-146a-5p mimic up-regulated DAD1 and IL8 gene expression in comparison to the LPS only group at each time point (Figure 16 and 17). LPS with miR-146a-5p mimic and LPS only groups both decreased at 1 and 8 hr, while increasing at 3 hr for DAD1 expression (Figure 16). LPS only and miR-146a-5p mimic with LPS had similar expression values at 0 hr and trends throughout the time course. However, the LPS only group had significantly decreased

values compared to the group with the mimic (Figure 16). IL8 expression showed that LPS with miR-146a-5p mimic and LPS only groups both decreased at 1 and 8 hr. However, at 3 hr for the mimic group with increased LPS concentration, there was no significant difference for the LPS only group at that timepoint (Figure 17). Additionally, insignificant value changes occurred from 1 to 8 hr for the LPS with miR-146a-5p mimic (Figure 17). Although the purpose of transfection of mimics is to typically reduce gene expression, this did not occur for miR-146a-5p mimic with LPS in DAD1 and IL8 expression. However, the expression trends for both DAD1 and IL8 genes indicate that miR-146a-5p may be indirectly involved in its regulation.

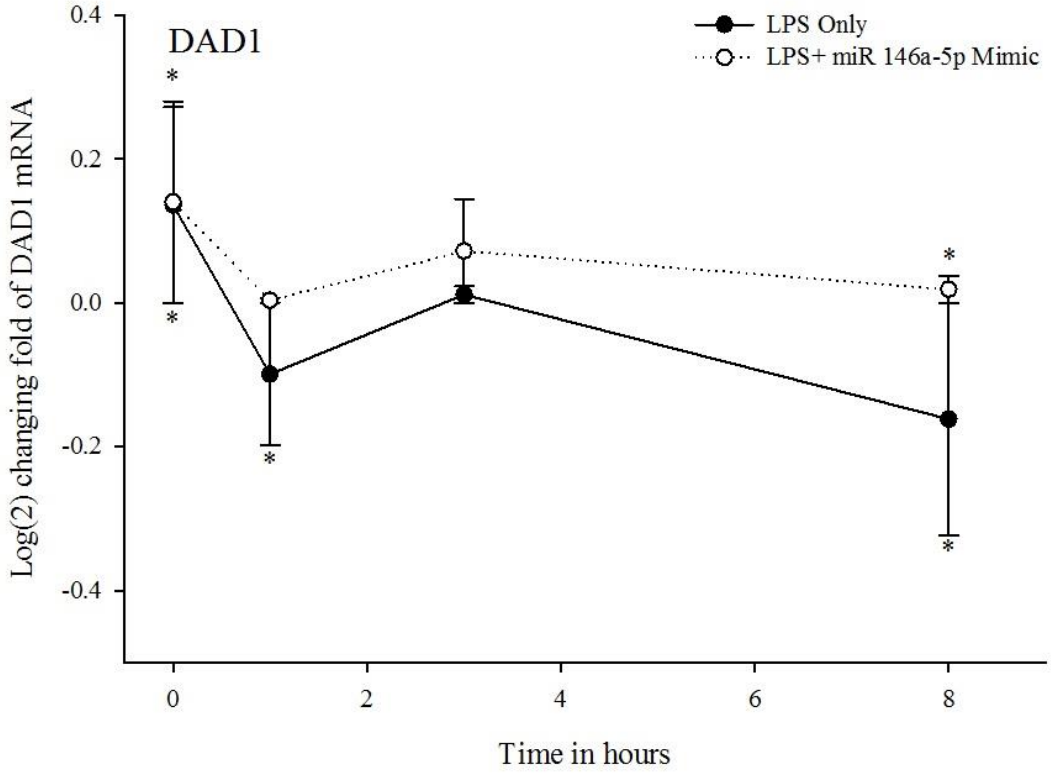

Figure 16. DAD1 gene expression with miR-146a-5p mimic. 1 μg/ml LPS stimulation or LPS stimulation with miR-146a-5p mimic at 0, 1, 3, and 8 hr for the mean gene expression of DAD1. The mean gene expression data is normalized against the temporal fold changes of its control group. Error bars represent the standard error of the mean (SEM). *Statistical differences based on the comparison of control at each corresponding time point (P>0.05)

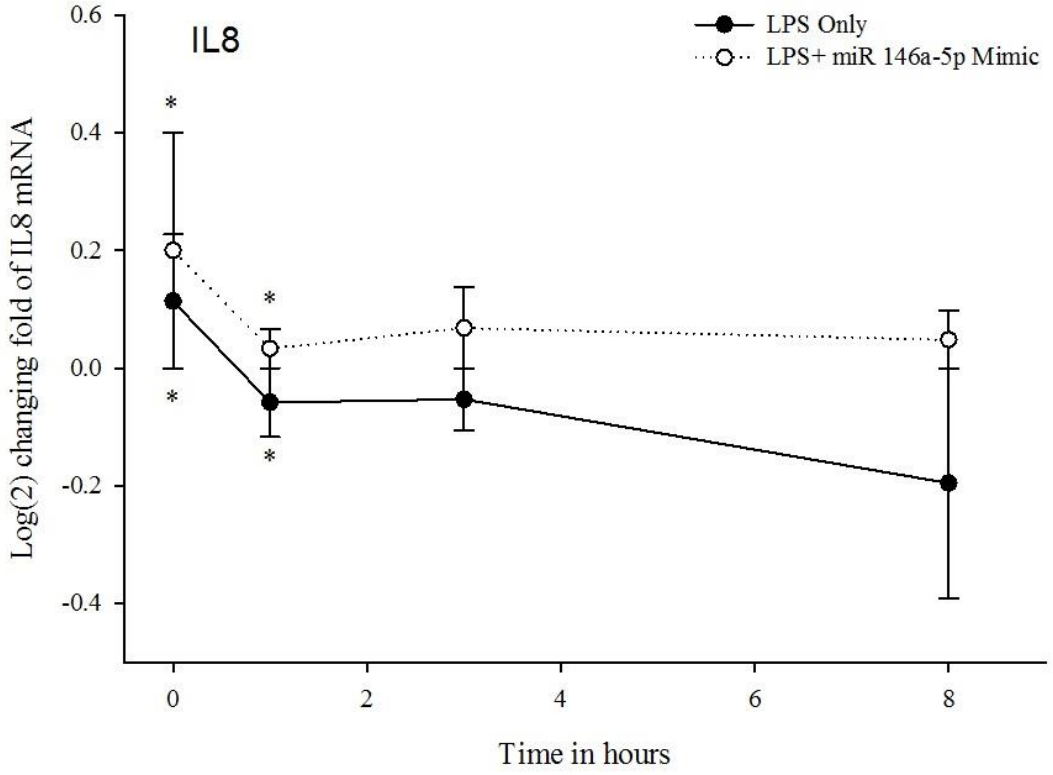

Figure 17. IL8 gene expression with miR-146a-5p mimic 1 μg/ml LPS stimulation or LPS stimulation with miR-146a-5p mimic at 0, 1, 3, and 8 hr for the mean gene expression IL8. The mean gene expression data is normalized against the temporal fold changes of its control group. Error bars represent the standard error of the mean (SEM). *Statistical differences based on the comparison of control at each corresponding time point (P>0.05)

Inverse regulatory relationship of let-7a-5p and DAD1

Initially after the LPS stimulation let-7a-5p mimic was upregulated compared to the LPS only group at 0 hr (Figure 18). LPS only group showed a decrease at 1 and 3 hr compared to an increase with the mimic at the same timepoint for DAD1. Furthermore, the gene expression decreased for DAD1 with LPS with mimic, while the expression increased for the LPS only group at 8 hr. However, for both groups

similar fold changes were observed at 8 hr for DAD1, and only marginal changes with the LPS only group (Figure 18). The expression levels varied inversely at each timepoint except for 3 hr. At the 3 hr point, the mimic with LPS exhibited larger changes compared to the LPS only group (Figure 18). The correlation between LPS and the transfection of let-7a-5p mimic may provide evidence for the impact of let-7a and its DAD1 target as a function of time. The DAD1 gene expression results show an inverse relationship between the LPS only group and the let-7a-5p mimic with LPS.

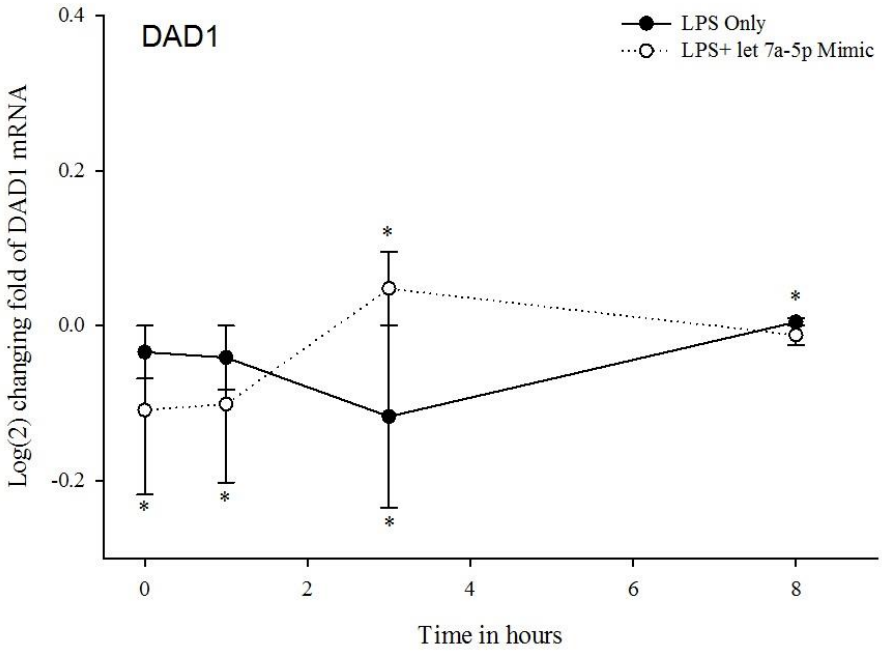

Figure 18. DAD1 gene expression with let-7a-5p mimic. DAD1 mean gene expression at 0, 1, 3, and 8 hr after 1 μg/ml LPS stimulation or LPS stimulation with let-7a-5p mimic (B). The mean gene expression data is normalized against the temporal fold changes of its control group. Error bars represent the standard error of the mean (SEM). *Statistical differences based on the comparison to the comparison of control at each corresponding time point (P>0.05).

Discussion

To understand the complexities of miRNA functionality, investigating the expression patterns within specific cell types is important in determining its role in disease and biological processes. Due to the lack of experimental data for miRNA in swine, the use of computational prediction tools based on sequences were solely used to identify potential mRNA targets (Riffo-Campos, Riquelme, & Brebi-Mieville, 2016). Although the sequences of the swine miRNAs of interest in the study are homologous to mature miRNAs in humans, further research was needed to confirm their predicted functions in swine. A single mRNA can be controlled by several different miRNAs. Previous research has shown that miRNAs can be involved in a variety of cellular processes such as apoptosis, cell growth and inflammation (He et al., 2020; Pileczki, Cojocneanu-Petric, Maralani, Neagoe, & Sandulescu, 2016; Sun et al., 2020).

In this study, an *in vitro* model of a selected number of miRNA mimic transfections was used to evaluate the regulation of DAD1, Il-8, ESR1 after LPS stimulation. Based on current research and confirmation from this study, we propose pathway model of the miRNAs of interest with each target to highlight their role in the inflammation process (Illustration 3). DAD1, also known as Defender Against Cell Death 1, is a known negative regulator of programmed cell death (Yan et al., 2019). The activation of the JNK signaling pathway and the reduction of tissue growth can be caused by the loss of DAD1 functionality (Y. Zhang, Cui, & Lai, 2016). In humans, increased DAD1 expression levels have been demonstrated in

subjects with asthma, which is considered a chronic inflammation of the airways (Pires et al., 2018). In the comparison between LPS only and LPS with miR-22-3p, the DAD1 gene expression demonstrated up-regulation in the LPS only group, consistent with previous findings (Hong, Kabra, Hsieh, Cado, & Winoto, 1999; Pires et al., 2018). The down-regulation of miR-22-3p is associated with an up-regulation of the Sirtuin1 (SIRT1) gene, which then reduces inflammation in adipose cells. Previously it was unclear if DAD1 is a target for miR-22-3p in human studies. However, the reduction of gene expression by this mimic is an indicator of its potential role in inflammatory regulation in swine tissues.

In the human monocytic cell THP-1 after LPS induction, the miR-146a expression levels were elevated through the NF-kβ signaling pathway (K. D. Taganov, M. P. Boldin, K.-J. Chang, & D. Baltimore, 2006). Additionally, inflammation studies in mice have shown that that LPS in the airways of mice results in neutrophil recruitment as well as increased miR-146a expression in the lungs (Moschos et al., 2007). The results from this study with the miR-146a-5p mimic showed a down-regulation for the ESR1 and up-regulation for DAD1 and IL8 gene expression after LPS induction. ESR1, which is responsible for the growth of cells and involved in regulatory functions in cardiovascular systems, was decreased after LPS stimulation in mouse endothelial cell lines (Holm, Andersson, Nordstrom, Hellstrand, & Nilsson, 2010). IL8 gene expression in neutrophils are known to increase after LPS induction and after tissue injury induced-inflammation (Fujishima

et al., 1993; X.-M. Wang, Hamza, Wu, & Dionne, 2009). Although our current data demonstrates miR-146a-5p may indirectly regulate DAD1 and IL8, it does not confirm its direct involvement in the regulation of ESR1 gene. Genes can also be upregulated by miRNAs if they share have a common transcription factor or are inhibited by an upstream suppressor (Tan et al., 2019). Further investigations are required to help extensively understand the precise targets and pathways that are up-regulated by these miRNAs. The let-7 miRNA family has a known role in inflammatory response; let-7a expression has been shown to be increased by LPS stimulation in the mouse cell line ATDC5 (Sui, Zhang, & Hu, 2019). The inverse relationship for the LPS and let-7 mimic group and the LPS only group has not been demonstrated in previous studies.

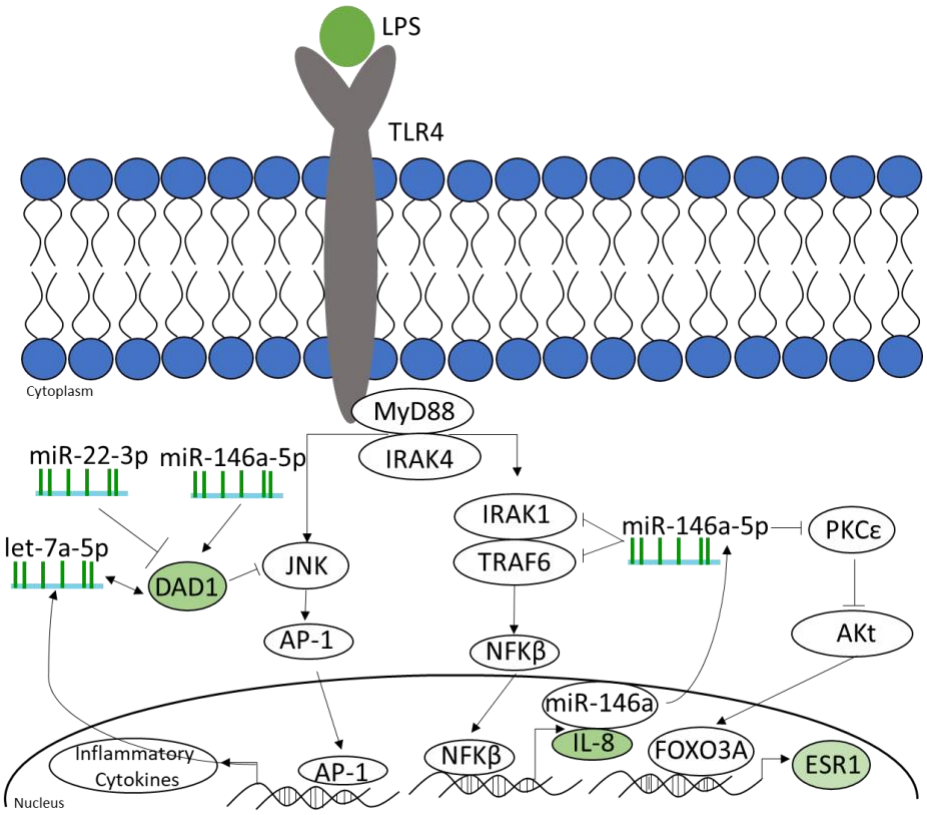

Illustration 3. Proposed swine miRNA pathways. The proposed scheme depicts the swine miRNAs of interest targeting a variety of inflammation molecules within a cell after LPS induction. In the inflammatory pathway of NF-kβ, mir-146a is involved in a negative feedback loop that inhibits IRAK1 and TRAF6. Protein kinase C (*PKCε)* is also inhibited by mir-146a, then inhibits the activation of Protein Kinase B (AKt) and downstream leads to the inhibition of ESR1. DAD1 is upregulated by both anti-inflammatory miR-146a-5p and miR-22-3p miRNAs which inhibits inflammatory cytokines. The inverse relationship between let-7a-5p and DAD1 has not been previously established and although the mechanism is not clear, it appears to be a negative feedback loop.

Chapter 7: Conclusions

The identification of a potential biological marker or combination of biomarkers to be accurately measured within food animals is essential. Initially, the goal was to determine the inflammatory induced changes in protein and miRNA expressions that correlate with the severity of the host's inflammatory response. The results showed an endotoxemic response in the swine and not a moderate inflammatory response as expected. Although this impeded the ability to demonstrate the changes for only inflammation, it provided an opportunity to determine if a surrogate protein or miRNA biomarkers can discriminate between inflammation and endotoxemia. Based on our research, the following potential outcomes can be enumerated:

1. Identifying and assessing the expression of unique small protein in swine inflammation was challenging for proteomic biomarkers. Due to the complexity of the sample and the high abundant proteins overshadowing numerous proteins, these limitations were a barrier that prevented additional protein analysis.
2. Our results suggested ssc-let-7e-5p and ssc-miR-22-3p miRNAs have the capability of discriminating between inflammation and endotoxemia. Additionally, ssc-miR-146a-5p expression levels indicated it can be a potential biomarker candidate for inflammatory responses.
3. Provided mRNA gene data that indicate the different expression patterns between control group and LPS stimulation as well as the impact of miRNA

overexpression by mimics. New evidence on the mRNA inflammatory profiles of DAD1, Il-8, ESR1 and confirmation of regulation by miRNAs expression in swine.

4. The molecular markers of mRNA and the expression of the ssc-let-7a-5p, ssc-miR-22-3p and ssc-miR-146a-5p may potentially be used to diagnose or treat inflammation.

In conclusion, the results of these studies showed a specific pattern of circulating miRNA plasma with inflammation on a time course, which can be used to determine its severity in swine. The analysis of the experimental miRNA-mRNA interactions provided additional verification based on computational database. The information gathered from this study will aid future *in vivo* studies as well as drug development in swine. This information will allow drug sponsors to provide biological evidence that their drug controls inflammation or the ability to produce a commercially available miRNA kit to assess the severity of inflammation within swine.

Bibliography

Abdelfattah, A. M., Park, C., & Choi, M. Y. (2014). Update on non-canonical microRNAs. *Biomolecular concepts, 5*(4), 275-287. doi:10.1515/bmc-2014-0012

Alexander, M., & O'Connell, R. M. (2015). Noncoding RNAs and chronic inflammation: Micro-managing the fire within. *Bioessays, 37*(9), 1005-1015. doi:10.1002/bies.201500054

Almeida, M. I., Reis, R. M., & Calin, G. A. (2011). MicroRNA history: discovery, recent applications, and next frontiers. *Mutat Res, 717*(1-2), 1-8. doi:10.1016/j.mrfmmm.2011.03.009

Androulidaki, A., Iliopoulos, D., Arranz, A., Doxaki, C., Schworer, S., Zacharioudaki, V., . . . Tsatsanis, C. (2009). The kinase Akt1 controls macrophage response to lipopolysaccharide by regulating microRNAs. *Immunity, 31*(2), 220-231. doi:10.1016/j.immuni.2009.06.024

Anon. (2004). Supplemental New Animal Drug Application for NADA 101-479 for Dairy Cattle for Claim to Treat Inflammation. Retrieved from http://www.fda.gov/downloads/AnimalVeterinary/Products/ApprovedAnimalDrugProducts/FOIADrugSummaries/ucm064910.pdf

Ardekani, A. M., & Naeini, M. M. (2010). The Role of MicroRNAs in Human Diseases. *Avicenna J Med Biotechnol, 2*(4), 161-179.

Asgari, S. (2011). Role of MicroRNAs in Insect Host–Microorganism Interactions. *Frontiers in Physiology, 2*(48). doi:10.3389/fphys.2011.00048

Bandow, J. E. (2010). Comparison of protein enrichment strategies for proteome analysis of plasma. *Proteomics, 10*(7), 1416-1425. doi:10.1002/pmic.200900431

Bartel, D. P. (2018). Metazoan MicroRNAs. *Cell, 173*(1), 20-51. doi:https://doi.org/10.1016/j.cell.2018.03.006

Biomarkers and surrogate endpoints: preferred definitions and conceptual framework. (2001). *Clin Pharmacol Ther, 69*(3), 89-95. doi:10.1067/mcp.2001.113989

Boehmer, J. L. (2011). Proteomic analyses of host and pathogen responses during bovine mastitis. *Journal of mammary gland biology and neoplasia, 16*(4), 323-338. doi:10.1007/s10911-011-9229-x

Boehmer, J. L., Ward, J. L., Peters, R. R., Shefcheck, K. J., McFarland, M. A., & Bannerman, D. D. (2010). Proteomic analysis of the temporal expression of bovine milk proteins during coliform mastitis and label-free relative quantification. *J Dairy Sci, 93*(2), 593-603. doi:10.3168/jds.2009-2526

Brennan, E., Wang, B., McClelland, A., Mohan, M., Marai, M., Beuscart, O., . . . Kantharidis, P. (2017). Protective Effect of let-7 miRNA Family in Regulating Inflammation in Diabetes-Associated Atherosclerosis. *Diabetes, 66*(8), 2266-2277. doi:10.2337/db16-1405

Brennecke, J., Stark, A., Russell, R. B., & Cohen, S. M. (2005). Principles of microRNA-target recognition. *PLoS biology, 3*(3), e85-e85. doi:10.1371/journal.pbio.0030085

Carthew, R. W., & Sontheimer, E. J. (2009). Origins and Mechanisms of miRNAs and siRNAs. *Cell, 136*(4), 642-655. doi:10.1016/j.cell.2009.01.035

Charlie-Silva, I., Klein, A., Gomes, J. M. M., Prado, E. J. R., Moraes, A. C., Eto, S. F., . . . Belo, M. A. A. (2019). Acute-phase proteins during inflammatory reaction by bacterial infection: Fish-model. *Scientific Reports, 9*(1), 4776. doi:10.1038/s41598-019-41312-z

Chen, B., Luo, L., Zhu, W., Wei, X., Li, S., Huang, Y., . . . Lin, X. (2016). miR-22 contributes to the pathogenesis of patients with coronary artery disease by targeting MCP-1: An observational study. *Medicine (Baltimore), 95*(33), e4418. doi:10.1097/md.0000000000004418

Chen, Y., & Wang, X. (2020). miRDB: an online database for prediction of functional microRNA targets. *Nucleic Acids Res, 48*(D1), D127-D131. doi:10.1093/nar/gkz757

Dharap, A., Pokrzywa, C., Murali, S., Pandi, G., & Vemuganti, R. (2013). MicroRNA miR-324-3p induces promoter-mediated expression of RelA gene. *PLoS One, 8*(11), e79467-e79467. doi:10.1371/journal.pone.0079467

Doi, K., Leelahavanichkul, A., Yuen, P. S., & Star, R. A. (2009). Animal models of sepsis and sepsis-induced kidney injury. *J Clin Invest, 119*(10), 2868-2878. doi:10.1172/jci39421

Fujishima, S., Hoffman, A. R., Vu, T., Kim, K. J., Zheng, H., Daniel, D., . . . Raffin, T. A. (1993). Regulation of neutrophil interleukin 8 gene expression and protein secretion by LPS, TNF-alpha, and IL-1 beta. *J Cell Physiol, 154*(3), 478-485. doi:10.1002/jcp.1041540305

Gabay, C., & Kushner, I. (1999). Acute-Phase Proteins and Other Systemic Responses to Inflammation. *New England Journal of Medicine, 340*(6), 448-454. doi:10.1056/nejm199902113400607

Gallo, A., Tandon, M., Alevizos, I., & Illei, G. G. (2012). The majority of microRNAs detectable in serum and saliva is concentrated in exosomes. *PLoS One, 7*(3), e30679. doi:10.1371/journal.pone.0030679

Gidlof, O., Sathanoori, R., Magistri, M., Faghihi, M. A., Wahlestedt, C., Olde, B., & Erlinge, D. (2015). Extracellular Uridine Triphosphate and Adenosine Triphosphate Attenuate Endothelial Inflammation through miR-22-Mediated ICAM-1 Inhibition. *J Vasc Res, 52*(2), 71-80. doi:10.1159/000431367

Giglio, S., Monis, P. T., & Saint, C. P. (2003). Demonstration of preferential binding of SYBR Green I to specific DNA fragments in real-time multiplex PCR. *Nucleic Acids Res, 31*(22), e136-e136. doi:10.1093/nar/gng135

Gilad, S., Meiri, E., Yogev, Y., Benjamin, S., Lebanony, D., Yerushalmi, N., . . . Chajut, A. (2008). Serum microRNAs are promising novel biomarkers. *PLoS One, 3*(9), e3148. doi:10.1371/journal.pone.0003148

Glinge, C., Clauss, S., Boddum, K., Jabbari, R., Jabbari, J., Risgaard, B., . . . Tfelt-Hansen, J. (2017). Stability of Circulating Blood-Based MicroRNAs - Pre-Analytic Methodological Considerations. *PLoS One, 12*(2), e0167969-e0167969. doi:10.1371/journal.pone.0167969

Gorg, A., Weiss, W., & Dunn, M. J. (2004). Current two-dimensional electrophoresis technology for proteomics. *Proteomics, 4*(12), 3665-3685. doi:10.1002/pmic.200401031

Gu, W., Zhan, H., Zhou, X. Y., Yao, L., Yan, M., Chen, A., . . . Liu, G. (2017). MicroRNA-22 regulates inflammation and angiogenesis via targeting VE-cadherin. *FEBS Lett, 591*(3), 513-526. doi:10.1002/1873-3468.12565

Gudiksen, K. L., Gitlin, I., & Whitesides, G. M. (2006). Differentiation of proteins based on characteristic patterns of association and denaturation in solutions of SDS. *Proceedings of the National Academy of Sciences of the United States of America, 103*(21), 7968-7972. doi:10.1073/pnas.0602816103

Gül, F., Arslantaş, M. K., Cinel, İ., & Kumar, A. (2017). Changing Definitions of Sepsis. *Turkish journal of anaesthesiology and reanimation, 45*(3), 129-138. doi:10.5152/TJAR.2017.93753

Ha, M., & Kim, V. N. (2014). Regulation of microRNA biogenesis. *Nature Reviews Molecular Cell Biology, 15*(8), 509-524. doi:10.1038/nrm3838

Hammond, S. M. (2015). An overview of microRNAs. *Adv Drug Deliv Rev, 87*, 3-14. doi:10.1016/j.addr.2015.05.001

He, W., Huang, Y., Jiang, C. C., Zhu, Y., Wang, L., Zhang, W., . . . Tang, S. (2020). miR-100 Inhibits Cell Growth and Proliferation by Targeting HOXA1 in Nasopharyngeal Carcinoma. *Onco Targets Ther, 13*, 593-602. doi:10.2147/ott.S228783

Holm, A., Andersson, K. E., Nordstrom, I., Hellstrand, P., & Nilsson, B. O. (2010). Down-regulation of endothelial cell estrogen receptor expression by the inflammation promoter LPS. *Mol Cell Endocrinol, 319*(1-2), 8-13. doi:10.1016/j.mce.2010.01.002

Hong, N. A., Kabra, N. H., Hsieh, S. N., Cado, D., & Winoto, A. (1999). In vivo overexpression of Dad1, the defender against apoptotic death-1, enhances T cell proliferation but does not protect against apoptosis. *J Immunol, 163*(4), 1888-1893.

Huang, H., Zhu, Y., & Li, S. (2015). MicroRNA-122 mimic transfection contributes to apoptosis in HepG2 cells. *Molecular medicine reports, 12*(5), 6918-6924. doi:10.3892/mmr.2015.4254

Hulanicka, M., Garncarz, M., Parzeniecka-Jaworska, M., & Jank, M. (2014). Plasma miRNAs as potential biomarkers of chronic degenerative valvular disease in Dachshunds. *BMC Vet Res, 10*, 205. doi:10.1186/s12917-014-0205-8

Iftikhar, H., & Carney, G. E. (2016). Evidence and potential in vivo functions for biofluid miRNAs: From expression profiling to functional testing: Potential roles of extracellular miRNAs as indicators of physiological change and as agents of intercellular information exchange. *Bioessays, 38*(4), 367-378. doi:10.1002/bies.201500130

Ito, K. (2007). Impact of post-translational modifications of proteins on the inflammatory process. *Biochem Soc Trans, 35*(Pt 2), 281-283. doi:10.1042/bst0350281

Jain, S., Gautam, V., & Naseem, S. (2011). Acute-phase proteins: As diagnostic tool. *Journal of pharmacy & bioallied sciences, 3*(1), 118-127. doi:10.4103/0975-7406.76489

Jayashree, B., Bibin, Y. S., Prabhu, D., Shanthirani, C. S., Gokulakrishnan, K., Lakshmi, B. S., . . . Balasubramanyam, M. (2014). Increased circulatory levels of lipopolysaccharide (LPS) and zonulin signify novel biomarkers of

proinflammation in patients with type 2 diabetes. *Mol Cell Biochem, 388*(1-2), 203-210. doi:10.1007/s11010-013-1911-4

Jiang, Z. F., Zhang, L., & Shen, J. (2020). MicroRNA: Potential biomarker and target of therapy in acute lung injury. *Hum Exp Toxicol, 39*(11), 1429-1442. doi:10.1177/0960327120926254

Jin, H. Y., & Xiao, C. (2015). MicroRNA Mechanisms of Action: What have We Learned from Mice? *Frontiers in genetics, 6*, 328-328. doi:10.3389/fgene.2015.00328

Klosterhalfen, B., Horstmann-Jungemann, K., Vogel, P., Dufhues, G., Simon, B., Kalff, G., . . . Heinrich, P. C. (1991). Hemodynamic variables and plasma levels of PGI2, TXA2 and IL-6 in a porcine model of recurrent endotoxemia. *Circ Shock, 35*(4), 237-244.

Kozomara, A., Birgaoanu, M., & Griffiths-Jones, S. (2018). miRBase: from microRNA sequences to function. *Nucleic Acids Res, 47*(D1), D155-D162. doi:10.1093/nar/gky1141

Kritselis, I., Tzanetakou, V., Adamis, G., Anthopoulos, G., Antoniadou, E., Bristianou, M., . . . Giamarellos-Bourboulis, E. J. (2013). The level of endotoxemia in sepsis varies in relation to the underlying infection: Impact on final outcome. *Immunol Lett, 152*(2), 167-172. doi:10.1016/j.imlet.2013.05.013

Kroh, E. M., Parkin, R. K., Mitchell, P. S., & Tewari, M. (2010). Analysis of circulating microRNA biomarkers in plasma and serum using quantitative reverse transcription-PCR (qRT-PCR). *Methods, 50*(4), 298-301. doi:10.1016/j.ymeth.2010.01.032

Kumar, M., Ahmad, T., Sharma, A., Mabalirajan, U., Kulshreshtha, A., Agrawal, A., & Ghosh, B. (2011). Let-7 microRNA-mediated regulation of IL-13 and allergic airway inflammation. *J Allergy Clin Immunol, 128*(5), 1077-1085.e1071-1010. doi:10.1016/j.jaci.2011.04.034

Lampreave, F., González-Ramón, N., Martínez-Ayensa, S., Hernández, M. A., Lorenzo, H. K., García-Gil, A., & Piñeiro, A. (1994). Characterization of the acute phase serum protein response in pigs. *Electrophoresis, 15*(5), 672-676. doi:10.1002/elps.1150150195

Lee, R. C., Feinbaum, R. L., & Ambros, V. (1993). The C. elegans heterochronic gene lin-4 encodes small RNAs with antisense complementarity to lin-14. *Cell, 75*(5), 843-854. doi:10.1016/0092-8674(93)90529-y

Lin, Z., Ge, J., Wang, Z., Ren, J., Wang, X., Xiong, H., . . . Zhang, Q. (2017). Let-7e modulates the inflammatory response in vascular endothelial cells through ceRNA crosstalk. *Scientific Reports, 7*(1), 42498. doi:10.1038/srep42498

Lippolis, J. D., & Reinhardt, T. A. (2010). Utility, limitations, and promise of proteomics in animal science. *Vet Immunol Immunopathol, 138*(4), 241-251. doi:10.1016/j.vetimm.2010.10.003

Livak, K. J., & Schmittgen, T. D. (2001). Analysis of Relative Gene Expression Data Using Real-Time Quantitative PCR and the 2−ΔΔCT Method. *Methods, 25*(4), 402-408. doi:https://doi.org/10.1006/meth.2001.1262

Maldonado, R. F., Sá-Correia, I., & Valvano, M. A. (2016). Lipopolysaccharide modification in Gram-negative bacteria during chronic infection. *FEMS microbiology reviews, 40*(4), 480-493. doi:10.1093/femsre/fuw007

Marshall, J. C., & Reinhart, K. (2009). Biomarkers of sepsis. *Crit Care Med, 37*(7), 2290-2298. doi:10.1097/CCM.0b013e3181a02afc

McFarland, M. A., Ellis, C. E., Markey, S. P., & Nussbaum, R. L. (2008). Proteomics analysis identifies phosphorylation-dependent alpha-synuclein protein interactions. *Molecular & cellular proteomics : MCP, 7*(11), 2123-2137. doi:10.1074/mcp.M800116-MCP200

Millner, L. M., & Strotman, L. N. (2016). The Future of Precision Medicine in Oncology. *Clin Lab Med, 36*(3), 557-573. doi:10.1016/j.cll.2016.05.003

Minden, J. (2007). Comparative proteomics and difference gel electrophoresis. *Biotechniques, 43*(6), 739, 741, 743 passim. doi:10.2144/000112653

Moschos, S. A., Williams, A. E., Perry, M. M., Birrell, M. A., Belvisi, M. G., & Lindsay, M. A. (2007). Expression profiling in vivo demonstrates rapid changes in lung microRNA levels following lipopolysaccharide-induced inflammation but not in the anti-inflammatory action of glucocorticoids. *BMC Genomics, 8*, 240. doi:10.1186/1471-2164-8-240

Myers, M. J., Scott, M. L., Deaver, C. M., Farrell, D. E., & Yancy, H. F. (2010). Biomarkers of inflammation in cattle determining the effectiveness of anti-inflammatory drugs. *Journal of Veterinary Pharmacology and Therapeutics, 33*(1), 1-8. doi:10.1111/j.1365-2885.2009.01096.x

Myers, M. J., Smith, E. R., & Turfle, P. G. (2017). Biomarkers in Veterinary Medicine. *Annu Rev Anim Biosci, 5*, 65-87. doi:10.1146/annurev-animal-021815-111431

Nemzek, J. A., Hugunin, K. M., & Opp, M. R. (2008). Modeling sepsis in the laboratory: merging sound science with animal well-being. *Comp Med, 58*(2), 120-128.

Newman, M. A., Thomson, J. M., & Hammond, S. M. (2008). Lin-28 interaction with the Let-7 precursor loop mediates regulated microRNA processing. *RNA (New York, N.Y.), 14*(8), 1539-1549. doi:10.1261/rna.1155108

Noh, S. J., Miller, S. H., Lee, Y. T., Goh, S. H., Marincola, F. M., Stroncek, D. F., . . . Miller, J. L. (2009). Let-7 microRNAs are developmentally regulated in

circulating human erythroid cells. *J Transl Med, 7*, 98. doi:10.1186/1479-5876-7-98

O'Brien, J., Hayder, H., Zayed, Y., & Peng, C. (2018). Overview of MicroRNA Biogenesis, Mechanisms of Actions, and Circulation. *Frontiers in endocrinology, 9*, 402-402. doi:10.3389/fendo.2018.00402

O'Farrell, P. H. (1975). High resolution two-dimensional electrophoresis of proteins. *The Journal of biological chemistry, 250*(10), 4007-4021. Retrieved from https://pubmed.ncbi.nlm.nih.gov/236308

https://www.ncbi.nlm.nih.gov/pmc/articles/PMC2874754/

Okada, C., Yamashita, E., Lee, S. J., Shibata, S., Katahira, J., Nakagawa, A., . . . Tsukihara, T. (2009). A high-resolution structure of the pre-microRNA nuclear export machinery. *Science, 326*(5957), 1275-1279. doi:10.1126/science.1178705

Olumee-Shabon, Z., Chattopadhaya, C., & Myers, M. J. (2020). Proteomics profiling of swine serum following lipopolysaccharide stimulation. *Rapid Commun Mass Spectrom, 34*(7), e8639. doi:10.1002/rcm.8639

Olumee-Shabon, Z., Swain, T., Smith, E. A., Tall, E., & Boehmer, J. L. (2013). Proteomic analysis of differentially expressed proteins in caprine milk during experimentally induced endotoxin mastitis. *J Dairy Sci, 96*(5), 2903-2912. doi:10.3168/jds.2012-5956

Perez-Patiño, C., Barranco, I., Parrilla, I., Valero, M. L., Martinez, E. A., Rodriguez-Martinez, H., & Roca, J. (2016). Characterization of the porcine seminal plasma proteome comparing ejaculate portions. *J Proteomics, 142*, 15-23. doi:10.1016/j.jprot.2016.04.026

Person, M. D., Shen, J., Traner, A., Hensley, S. C., Lo, H.-H., Abbruzzese, J. L., & Li, D. (2006). Protein fragment domains identified using 2D gel electrophoresis/MALDI-TOF. *Journal of biomolecular techniques : JBT, 17*(2), 145-156. Retrieved from https://pubmed.ncbi.nlm.nih.gov/16741242 https://www.ncbi.nlm.nih.gov/pmc/articles/PMC2291776/

Peters, S. M., Yancy, H., Bremer, E., Monroe, J., Paul, D., Stubbs, J. T., 3rd, & Myers, M. J. (2011). In vitro identification and verification of inflammatory biomarkers in swine. *Vet Immunol Immunopathol, 139*(1), 67-72. doi:10.1016/j.vetimm.2010.08.001

Peters, S. M., Yancy, H., Deaver, C., Jones, Y. L., Kenyon, E., Chiesa, O. A., . . . Myers, M. J. (2012). In vivo characterization of inflammatory biomarkers in swine and the impact of flunixin meglumine administration. *Vet Immunol Immunopathol, 148*(3-4), 236-242. doi:10.1016/j.vetimm.2012.05.001

Pileczki, V., Cojocneanu-Petric, R., Maralani, M., Neagoe, I. B., & Sandulescu, R. (2016). MicroRNAs as regulators of apoptosis mechanisms in cancer. *Clujul Med, 89*(1), 50-55. doi:10.15386/cjmed-512

Pires, A. d. O., Queiroz, G. d. A., de Jesus Silva, M., da Silva, R. R., da Silva, H. B. F., Carneiro, N. V. Q., . . . Figueiredo, C. A. (2018). Polymorphisms in the DAD1 and OXA1L genes are associated with asthma and atopy in a South American population. *Molecular Immunology, 101*, 294-302. doi:https://doi.org/10.1016/j.molimm.2018.07.014

Ponchel, F., Toomes, C., Bransfield, K., Leong, F. T., Douglas, S. H., Field, S. L., . . . Markham, A. F. (2003). Real-time PCR based on SYBR-Green I fluorescence: an alternative to the TaqMan assay for a relative quantification of gene rearrangements, gene amplifications and micro gene deletions. *BMC biotechnology, 3*, 18-18. doi:10.1186/1472-6750-3-18

Pratt, A. J., & MacRae, I. J. (2009). The RNA-induced silencing complex: a versatile gene-silencing machine. *The Journal of biological chemistry, 284*(27), 17897-17901. doi:10.1074/jbc.R900012200

Punchard, N. A., Whelan, C. J., & Adcock, I. (2004). The Journal of Inflammation. *Journal of inflammation (London, England), 1*(1), 1-1. doi:10.1186/1476-9255-1-1

Puskarich, M. A., Nandi, U., Shapiro, N. I., Trzeciak, S., Kline, J. A., & Jones, A. E. (2015). Detection of microRNAs in patients with sepsis. *Journal of Acute Disease, 4*(2), 101-106. doi:https://doi.org/10.1016/S2221-6189(15)30017-2

Requião, R. D., Fernandes, L., de Souza, H. J. A., Rossetto, S., Domitrovic, T., & Palhano, F. L. (2017). Protein charge distribution in proteomes and its impact on translation. *PLoS computational biology, 13*(5), e1005549-e1005549. doi:10.1371/journal.pcbi.1005549

Ricciotti, E., & FitzGerald, G. A. (2011). Prostaglandins and Inflammation. *Arteriosclerosis, thrombosis, and vascular biology, 31*(5), 986-1000. doi:10.1161/atvbaha.110.207449

Rice, J., Roberts, H., Burton, J., Pan, J., States, V., Rai, S. N., & Galandiuk, S. (2015). Assay reproducibility in clinical studies of plasma miRNA. *PLoS One, 10*(4), e0121948. doi:10.1371/journal.pone.0121948

Riffo-Campos, Á. L., Riquelme, I., & Brebi-Mieville, P. (2016). Tools for Sequence-Based miRNA Target Prediction: What to Choose? *International journal of molecular sciences, 17*(12), 1987. doi:10.3390/ijms17121987

Ryan, G. B., & Majno, G. (1977). Acute inflammation. A review. *The American journal of pathology, 86*(1), 183-276. Retrieved from https://pubmed.ncbi.nlm.nih.gov/64118

https://www.ncbi.nlm.nih.gov/pmc/articles/PMC2032041/

Schluger, N. W., & Rom, W. N. (1995). The polymerase chain reaction in the diagnosis and evaluation of pulmonary infections. *Am J Respir Crit Care Med, 152*(1), 11-16. doi:10.1164/ajrccm.152.1.7599808

Seemann, S., Zohles, F., & Lupp, A. (2017). Comprehensive comparison of three different animal models for systemic inflammation. *J Biomed Sci, 24*(1), 60. doi:10.1186/s12929-017-0370-8

Signore, A., & Glaudemans, A. W. (2011). The molecular imaging approach to image infections and inflammation by nuclear medicine techniques. *Ann Nucl Med, 25*(10), 681-700. doi:10.1007/s12149-011-0521-z

Stortz, J. A., Raymond, S. L., Mira, J. C., Moldawer, L. L., Mohr, A. M., & Efron, P. A. (2017). Murine Models of Sepsis and Trauma: Can We Bridge the Gap? *ILAR journal, 58*(1), 90-105. doi:10.1093/ilar/ilx007

Strimbu, K., & Tavel, J. A. (2010). What are biomarkers? *Current opinion in HIV and AIDS, 5*(6), 463-466. doi:10.1097/COH.0b013e32833ed177

Sui, C., Zhang, L., & Hu, Y. (2019). MicroRNA-let-7a inhibition inhibits LPS-induced inflammatory injury of chondrocytes by targeting IL6R. *Molecular medicine reports, 20*(3), 2633-2640. doi:10.3892/mmr.2019.10493

Sun, F., Li, S. G., Zhang, H. W., Hua, F. W., Sun, G. Z., & Huang, Z. (2020). MiRNA-411 attenuates inflammatory damage and apoptosis following spinal cord injury. *Eur Rev Med Pharmacol Sci, 24*(2), 491-498. doi:10.26355/eurrev_202001_20022

Swain, T., Deaver, C., Lewandowski, A., & Myers, M. J. (Manuscript submitted for publication). Lipopolysaccharide (LPS) induced inflammatory changes in miRNA expression correlates to the severity of the host inflammatory response.

Taganov, K. D., Boldin, M. P., Chang, K.-J., & Baltimore, D. (2006). NF-kappaB-dependent induction of microRNA miR-146, an inhibitor targeted to signaling proteins of innate immune responses. *Proceedings of the National Academy of Sciences of the United States of America, 103*(33), 12481-12486. doi:10.1073/pnas.0605298103

Taganov, K. D., Boldin, M. P., Chang, K. J., & Baltimore, D. (2006). NF-kappaB-dependent induction of microRNA miR-146, an inhibitor targeted to signaling proteins of innate immune responses. *Proceedings of the National Academy of Sciences of the United States of America, 103*(33), 12481-12486. doi:10.1073/pnas.0605298103

Tan, H., Huang, S., Zhang, Z., Qian, X., Sun, P., & Zhou, X. (2019). Pan-cancer analysis on microRNA-associated gene activation. *EBioMedicine, 43*, 82-97. doi:10.1016/j.ebiom.2019.03.082

Timoneda, O., Nunez-Hernandez, F., Balcells, I., Munoz, M., Castello, A., Vera, G., . . . Nunez, J. I. (2014). The role of viral and host microRNAs in the Aujeszky's

disease virus during the infection process. *PLoS One, 9*(1), e86965. doi:10.1371/journal.pone.0086965

Turchinovich, A., Weiz, L., & Burwinkel, B. (2012). Extracellular miRNAs: the mystery of their origin and function. *Trends Biochem Sci, 37*(11), 460-465. doi:10.1016/j.tibs.2012.08.003

Valones, M. A. A., Guimarães, R. L., Brandão, L. A. C., de Souza, P. R. E., de Albuquerque Tavares Carvalho, A., & Crovela, S. (2009). Principles and applications of polymerase chain reaction in medical diagnostic fields: a review. *Brazilian journal of microbiology : [publication of the Brazilian Society for Microbiology], 40*(1), 1-11. doi:10.1590/S1517-83822009000100001

Van Amersfoort, E. S., Van Berkel, T. J., & Kuiper, J. (2003). Receptors, mediators, and mechanisms involved in bacterial sepsis and septic shock. *Clin Microbiol Rev, 16*(3), 379-414. doi:10.1128/cmr.16.3.379-414.2003

van Bragt, J., Vijverberg, S. J. H., Weersink, E. J. M., Richards, L. B., Neerincx, A. H., Sterk, P. J., . . . Maitland-van der Zee, A. H. (2018). Blood biomarkers in chronic airways diseases and their role in diagnosis and management. *Expert Rev Respir Med, 12*(5), 361-374. doi:10.1080/17476348.2018.1457440

Vargas-Caraveo, A., Sayd, A., Robledo-Montana, J., Caso, J. R., Madrigal, J. L. M., Garcia-Bueno, B., & Leza, J. C. (2020). Toll-like receptor 4 agonist and

antagonist lipopolysaccharides modify innate immune response in rat brain circumventricular organs. *J Neuroinflammation, 17*(1), 6. doi:10.1186/s12974-019-1690-2

Vlachos, I. S., Kostoulas, N., Vergoulis, T., Georgakilas, G., Reczko, M., Maragkakis, M., . . . Hatzigeorgiou, A. G. (2012). DIANA miRPath v.2.0: investigating the combinatorial effect of microRNAs in pathways. *Nucleic Acids Res, 40*(Web Server issue), W498-504. doi:10.1093/nar/gks494

Wang, J., Mei, J., & Ren, G. (2019). Plant microRNAs: Biogenesis, Homeostasis, and Degradation. *Frontiers in plant science, 10*, 360-360. doi:10.3389/fpls.2019.00360

Wang, L., Wang, H. C., Chen, C., Zeng, J., Wang, Q., Zheng, L., & Yu, H. D. (2013). Differential expression of plasma miR-146a in sepsis patients compared with non-sepsis-SIRS patients. *Exp Ther Med, 5*(4), 1101-1104. doi:10.3892/etm.2013.937

Wang, X.-M., Hamza, M., Wu, T.-X., & Dionne, R. A. (2009). Upregulation of IL-6, IL-8 and CCL2 gene expression after acute inflammation: Correlation to clinical pain. *Pain, 142*(3), 275-283. doi:10.1016/j.pain.2009.02.001

Wang, Z. (2011). The guideline of the design and validation of MiRNA mimics. *Methods Mol Biol, 676*, 211-223. doi:10.1007/978-1-60761-863-8_15

Wasinger, V. C., Cordwell, S. J., Cerpa-Poljak, A., Yan, J. X., Gooley, A. A., Wilkins, M. R., . . . Humphery-Smith, I. (1995). Progress with gene-product mapping of the Mollicutes: Mycoplasma genitalium. *Electrophoresis, 16*(7), 1090-1094. doi:10.1002/elps.11501601185

Weber, J. A., Baxter, D. H., Zhang, S., Huang, D. Y., Huang, K. H., Lee, M. J., . . . Wang, K. (2010). The microRNA spectrum in 12 body fluids. *Clinical chemistry, 56*(11), 1733-1741. doi:10.1373/clinchem.2010.147405

Werts, C., Tapping, R. I., Mathison, J. C., Chuang, T. H., Kravchenko, V., Saint Girons, I., . . . Ulevitch, R. J. (2001). Leptospiral lipopolysaccharide activates cells through a TLR2-dependent mechanism. *Nat Immunol, 2*(4), 346-352. doi:10.1038/86354

Wightman, B., Ha, I., & Ruvkun, G. (1993). Posttranscriptional regulation of the heterochronic gene lin-14 by lin-4 mediates temporal pattern formation in C. elegans. *Cell, 75*(5), 855-862. doi:10.1016/0092-8674(93)90530-4

Wulfkuhle, J. D., Liotta, L. A., & Petricoin, E. F. (2003). Proteomic applications for the early detection of cancer. *Nat Rev Cancer, 3*(4), 267-275. Retrieved from http://dx.doi.org/10.1038/nrc1043

Yan, Q., Si, J., Cui, X., Peng, H., Jing, M., Chen, X., . . . Dou, D. (2019). GmDAD1, a Conserved Defender Against Cell Death 1 (DAD1) From Soybean,

Positively Regulates Plant Resistance Against Phytophthora Pathogens. *Frontiers in plant science, 10*, 107-107. doi:10.3389/fpls.2019.00107

Yang, J.-S., & Lai, E. C. (2011). Alternative miRNA biogenesis pathways and the interpretation of core miRNA pathway mutants. *Molecular cell, 43*(6), 892-903. doi:10.1016/j.molcel.2011.07.024

Zhang, H., Kolb, F. A., Jaskiewicz, L., Westhof, E., & Filipowicz, W. (2004). Single processing center models for human Dicer and bacterial RNase III. *Cell, 118*(1), 57-68. doi:10.1016/j.cell.2004.06.017

Zhang, Y., Cui, C., & Lai, Z.-C. (2016). The defender against apoptotic cell death 1 gene is required for tissue growth and efficient N-glycosylation in Drosophila melanogaster. *Developmental Biology, 420*(1), 186-195. doi:https://doi.org/10.1016/j.ydbio.2016.09.021